




Paper based microfluidic devices: a review of fabrication techniques and applications

Anushka, Aditya Bandopadhyay^a , and Prasanta Kumar Das^b

Department of Mechanical Engineering, Indian Institute of Technology Kharagpur, Kharagpur, West Bengal 721302, India

Received 23 August 2022 / Accepted 9 November 2022 / Published online 12 December 2022

© The Author(s), under exclusive licence to EDP Sciences, Springer-Verlag GmbH Germany, part of Springer Nature 2022

Abstract A wide range of applications are possible with paper-based analytical devices, which are low priced, easy to fabricate and operate, and require no specialized equipment. Paper-based microfluidics offers the design of miniaturized POC devices to be applied in the health, environment, food, and energy sector employing the ASSURED (Affordable, Sensitive, Specific, User-friendly, Rapid and Robust, Equipment free and Deliverable to end users) principle of WHO. Therefore, this field is growing very rapidly and ample research is being done. This review focuses on fabrication and detection techniques reported to date. Additionally, this review emphasises on the application of this technology in the area of medical diagnosis, energy generation, environmental monitoring, and food quality control. This review also presents the theoretical analysis of fluid flow in porous media for the efficient handling and control of fluids. The limitations of PAD have also been discussed with an emphasis to concern on the transformation of such devices from laboratory to the consumer.

Abbreviations

PAD	Paper-based analytical device
μ PAD	Microfluidic paper-based analytical device
ePAD	Electrochemical Paper-based analytical device
PCAD	Microfluidic paper-based chemiluminescence analytical device
WHO	World health organisation
LOC	Lab-on-chip
LFA	Lateral flow assay
SPCE	Screen-printed carbon electrodes
PMMA	Poly methyl methacrylate
FLASH	Fast lithographic activation of sheets
PDMS	Polydimethylsiloxane
AKD	Alkyl ketene dime
LAMP	Loop-mediated isothermal amplification
RT-PCR	Real-time reverse transcription-polymerase chain reaction
RT-LAMP	Reverse transcription loop-mediated isothermal amplification

SARS-CoV Severe acute respiratory syndrome-associated coronavirus

ELISA Enzyme-linked immunosorbent assay

POC Point-of-care

1 Introduction

In microfluidics, fluids and particles are controlled and manipulated by precise equipment on scales of tens to hundreds of micrometers. Microfluidics leverages fluids in microchannels to exploit their most obvious characteristics small size and laminar flow. Microfluidics is also used for medical and chemical applications, such as lab-on-a-chips (LOC) and micro total analysis systems (μ TAS). This technology features superior advantages over conventional macro-scale platforms (e.g. centrifuges, flow cytometers, etc.) because it can precisely control and manipulate biological particles and the surrounding microenvironment.

Although microfluidics has been developing rapidly, the progression of POC microfluidic systems still faces various barriers like sample processing, chip to real-world connection, sensing, and miniaturization or abolition of additional fluid control elements. The difficulty

^ae-mail: aditya@mech.iitkgp.ac.in (corresponding author)

^be-mail: pkd@mech.iitkgp.ac.in

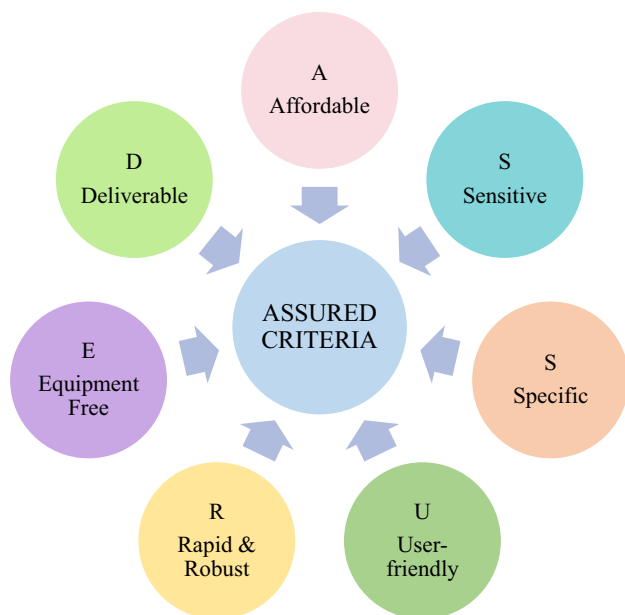


Fig. 1 An illustration of the WHO's ASSURED criteria for diagnostics

and high expenses of advancement of microfluidic products, make it difficult to reach end customers. Therefore, Martinez et al. [1] merged the concept of microfluidics with paper, as paper meets the optimal base material parameters for the transfer of these devices from the lab to consumers. These paper-based analytical devices (PADs) offer a separate site for liquid transportation via capillary forces without the use of additional pumps. Paper-based microfluidics is a rapidly growing field that has attracted significant attention due to its advantages over traditional microfluidics, such as low manufacturing costs, accessibility, ease of operation, scalability, fast response, POC diagnostics, and little solution usage. Therefore, this technology meets the guidelines of WHO for an ideal POC diagnostic system. Under WHO guidelines, the diagnostic test/device must meet the ASSURED requirements (as shown in Fig. 1) which include being (i) affordable, (ii) sensitive, (iii) specific, (iv) user-friendly, (v) rapid and robust, (vi) equipment-free, and (vii) deliverable to end-users for the selection of diagnostics [2, 3].

As a result, the field of testing is constantly developing and discovering new tools for identifying both infectious and non-infectious disorders. Incorporating microfluidics and biosensing principles can meet the criteria listed by the WHO here for choosing testing tools [3, 4]. In addition to satisfying the ASSURED criteria, microfluidic chip biosensors provide many additional advantages, such as portability, the need for fewer samples, the possibility of installation in rural parts, reduced energy consumption, less errors, numerous biomarker identification, etc.

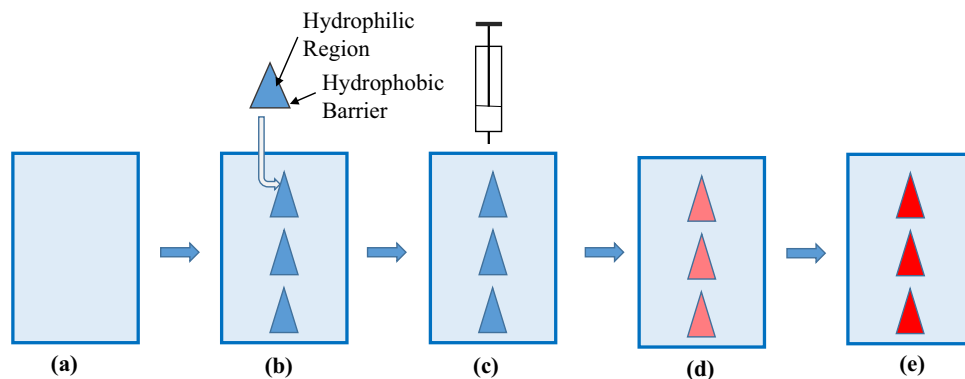
Creating channels is all that is necessary to execute multiplexed analysis by a succession of hydrophilic-hydrophobic microstructures on paper substrates to

create PADs. Photolithography, wax printing, screen printing, inkjet printing, and plasma oxidation are some of the common methods to create channels in the device. To improve the sensitivity and working of the device, certain modifications like the incorporation of the electrode were required. Colorimetric, chemiluminescence, and electrochemical techniques are employed for the goal of detection, and they entail the measurement of color intensity created on the PAD. Figure 2 shows a typical configuration for a paper-based microfluidic analytical device in which patterns were created on a simple Whatman filter paper to create the hydrophobic-hydrophilic contrast and then reagents and samples have been loaded to analyze the developed color in the reaction zone. There are many detection techniques have been explored including colorimetric analysis, fluorescent analysis, electrochemical analysis, etc. Colorimetric detection is a good method for μ PADs, which has the benefits of visual monitoring, quick sensing, practicality for rural applications, ease of use, and greater stability. In spite of improvements, there are still a few problems with paper-based microfluidic technology. The issues to take into account relate to the devices' stability and shelf life, particularly those that involve biological tests for analysis. The field of 'PADs' has experienced tremendous growth, but there are still many obstacles to overcome and possibilities to seize. The development of tools that are simpler to use must also continue. The complexity of assays for current technologies can be limited because of their intrinsic simplicity, or they can do complicated activities but are difficult to operate. This review explains the design and fabrication methods with various adjustments to generate practical assay with efficient handling and regulation of fluids, since μ PADs primary issue is the paucity of flow control, this slows down the process from the lab to the public hands and creates marketing challenges. Then it will transition to how these technologies carry out detection. The quantitative understanding of capillary flow was also revealed with various theoretical analysis of fluid flow in porous media. The Review will conclude with applications of PAD technology across medical diagnosis, environmental monitoring, energy generation, and food safety monitoring before concluding with a consideration of future directions of paper-based devices.

2 Fabrication

Like any other microfluidic system, fabrication is very important also for paper based device. The remarkable characteristics of paper have been the key to the development of PADs. There is no need to use external energy devices with paper-based microfluidics since it relies on capillary action to transfer liquids. Two basic steps are involved in creating μ PADs: Paper patterning and device customization to serve the purposes for which they are intended.

Fig. 2 PAD **a** filter paper, **b** patterned hydrophobic channels, **c** loading reagents, **d** loading sample, and **e** result



2.1 Patterning

Patterning is the first step in the fabrication of any PAD and is required to achieve hydrophilic-hydrophobic contrast in a porous paper. The two main patterning techniques for creating microfluidic channels on paper substrates are mechanical cutting and hydrophobic material treatment. Direct and indirect methods can be used to further categorize the second technique into two categories. In the direct technique, the hydrophobic material is applied directly to the paper, although for the indirect methods, the hydrophobic material is applied selectively at different stages using a mask, as indicated in Fig. 3. Wax printing, inkjet printing, flexographic printing, and laser cutting are examples of direct techniques while indirect method involves Plasma etching, photolithography, laser treatment, etc. The strategies of patterning principles can be separated based on the

binding states of the hydrophobic agent: (1) physically sealing the pores of the paper, (2) physically depositing a hydrophobizing substance on the cellulose fiber surfaces, and (3) chemically altering the surfaces of the fibers.

2.1.1 Photolithography

Photolithography was used to create the first paper-based microfluidic devices, and it continues to be preferable due to its accuracy and high resolution [5]. The photolithography begins by covering the complete paper with a negative photoresist as shown in Fig. 4. Moreover, the photoresist is crosslinked in the appropriate pattern by using a photomask. Finally, the substrate is developed in solvent to eliminate the remaining photoresist that hasn't been exposed [6, 7]. Martinez et al. [1] demonstrated the photolithography technique and used SU-8 2010 photoresist to create patterns on chromatography paper, then soaked and deposited the photoresist onto the paper. Now, the paper was baked for a few minutes to take off the cyclopentanone in the SU-8 formula. After that, a photo mask that had been precisely aligned with the aid of a mask aligner was used to expose the paper to UV light for couple of seconds. Although SU-8 is pricey and the procedure is complicated, the manufactured PADs have good resolution. Furthermore, Whitesides and colleagues used a SC photoresist [8] and an epoxy negative photoresist [9] for the SU-8 2010 photoresist.

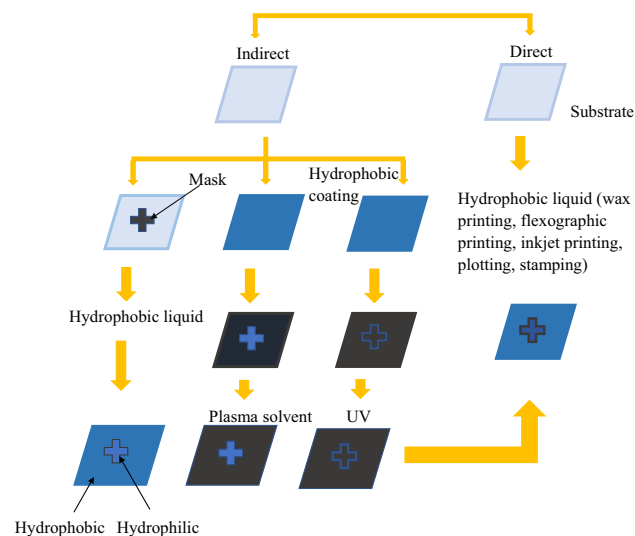
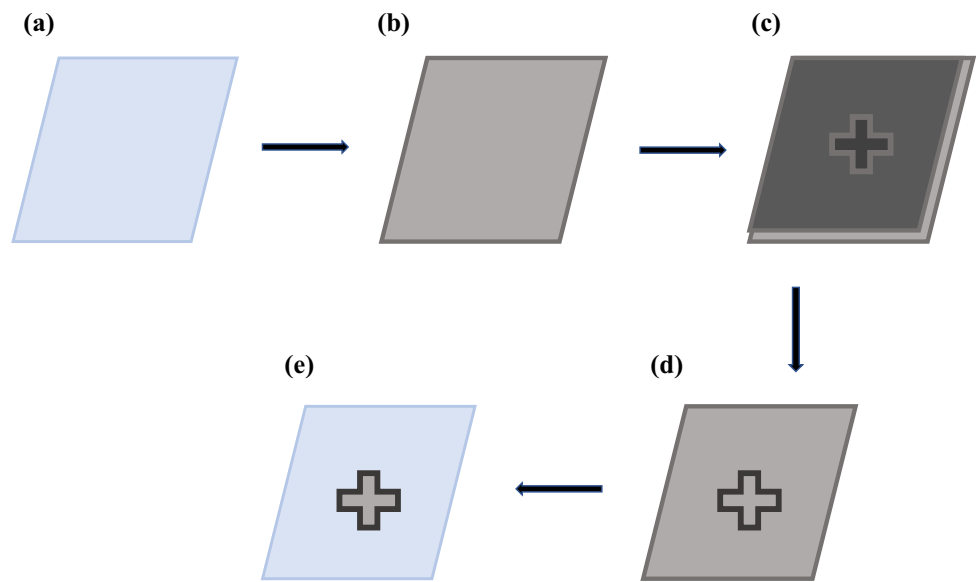


Fig. 3 Classification of patterning methods to form microfluidic channels. Patterning is classified based on the technique of transferring hydrophobic material on paper. If the hydrophobic material is applied directly to the hydrophilic paper substrate, it is called the direct method while if the hydrophobic material is applied selectively at different stages, it is the indirect method

2.1.2 Wax patterning

Wax is a hydrophobic substance that can be used on the hydrophobic surface using different ways. There are many benefits of using wax printing for the patterning of devices, including ease of fabrication, non-toxicity, disposability, and lower production costs. In 2009, Lu et al. [10] created a new wax impregnation process known as wax printing. Molten wax, as opposed to ink or toner, is imprinted on the surface of the paper by solid ink printers used for wax printing [11, 12]. Heat is applied to a piece of paper with a wax design

Fig. 4 Diagram showing the photolithography process. **a** Chromatography paper, **b** soaking the paper in a photoresist, **c** after prebaking aligning under a mask, **d** exposure to UV light, and **e** cleaning the developed pattern



printed on one side in order to flow the wax and permit it to reach the paper's thickness [13, 14]. This creates a hydrophobic barrier that is entirely impermeable and has a hydrophilic zone enclosed inside it that is shaped like a wax printing pattern. To prevent the reverse side of paper from becoming wet and to stop the permeation-related leakage of reagents and samples to the other side, a clear tape [15, 16] or laminated film is lastly applied to one side of the paper. While the wax is heated, it spreads both laterally and vertically, therefore this must be taken into consideration when drawing the designs. Channels of various sizes can be produced by printing wax in a variety of thicknesses or quantities.

2.1.3 Wax dipping

Compared to photolithography, it is a more expedient and economical printing method. It only requires wax dipping, and the channel was created in under a minute using subsequent soaking and standard heating techniques [13]. Hydrophobic barriers were created using melted wax, and hydrophilic channels were shielded using an iron mould as in Fig. 5. The magnetic field of a magnet was used to apply the iron mould to the paper. The paper absorbs the molten wax whenever the specimen is submerged in it, but some sections of the iron mould are shielded from the wax's absorption. The size of the iron mould that is used determines the precise width of the manufactured microfluidic channel.

2.1.4 Inkjet printing

In this method, a solvent is used in place of ink to pattern paper using a commercial inkjet printer. One application of this method involves first totally hydrophobizing paper by soaking it in a polystyrene solution. The paper is then treated with toluene inkjet printed in a

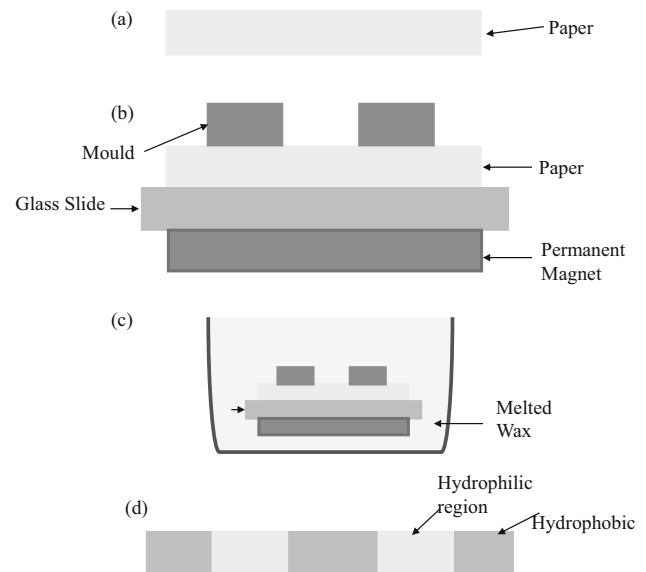
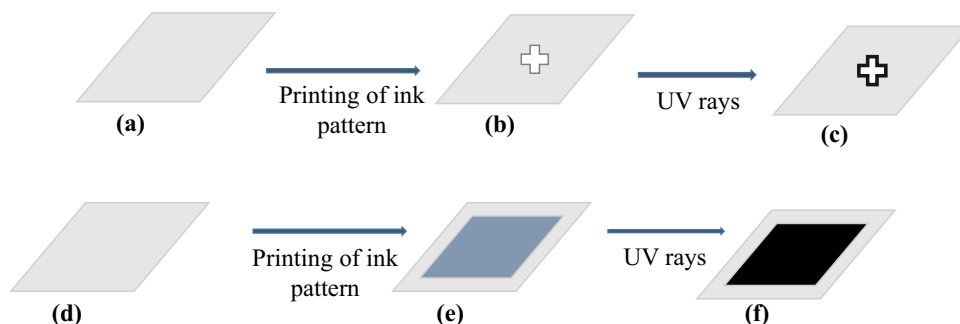


Fig. 5 Diagram showing the wax dipping process. **a** Filter Paper, **b** a magnet was mounted to the rear of a glass slide to generate an assembly of paper between a glass plate and a mould, **c** assembly was submerged in a wax chamber, **d** peeling off the glass plate and detaching the iron mould at room temperature resulted in the creation of the hydrophobic and hydrophilic regions of the μ PADs

specific pattern to remove some of the polystyrenes [17, 18]. The printers used for inkjet printing are relatively inexpensive and easily available and the reagents used for inkjet printing can directly print onto the device, helping in making an entire device in just one step. Abe et al. [18] used an inkjet-printed device for the sensing of glucose, proteins, and pH and proposed a method for creating mesoporous colloidal nanoparticle ink using an inkjet printer on both rigid and flexible substrates [19]. This technique permits sophisticated vapor responses

Fig. 6 Schematic diagram illustrating inkjet printing. **a** Top view of filter paper, **b** printing of ink pattern, **c** UV curing on the top side, **d** bottom view of filter paper, **e** printing of ink, **f** UV curing on the bottom side



for multiple-color PC patterns, and variations in color intensity have been seen with the unaided eye. Maejima et al. [20] created PADs using a similar inkjet printing technique. However, they substituted AKD in this instance with a hydrophobic UV curable acrylate composition made of non-volatile and non-flammable substances as shown in 6. After the unique ink had been printed on the paper, hydrophobic barriers were created by curing the material under UV light for 60 s [21]. The drawback of this method is that inkjet printing frequently necessitates the production of many printed layers and can result in print resolution issues. Since a large number of solvents used to emulsify detecting compounds are flammable, which might clog printers or result in errors in the quantity of reagents that are printed.

2.1.5 Laser treatment

The CO_2 laser is the most often utilized laser source for creating paper-based devices. Without support material to shield the material at the back, this can go into anything in a single pass. In order to create microfluidic devices, double-sided adhesive, PMMA, and paper are frequently sliced using a CO_2 laser while maintaining the specific value of operational parameters like the strength of the laser and the reading rate to prevent paper cutting. Mani et al. [22] reported a microchip to diagnose tuberculosis (TB) in the human body, which was framed using a laser cutting procedure. This TB ELISA is a fast, low-cost, and magnetically operated platform. The test duration could be halved to about 15 min while maintaining detection efficiencies on par with those of traditional, classical ELISA. Renault et al. [23] considerably enhanced the rate of flow of liquid on the porous chip and decreased nonspecific adsorption by cutting a channel with a laser to create an intermediate hollowed-out sandwich chip sensor (hollow channel). Chitnis et al. [24] proposed a laser-treated microfluidic device with the use of a substrate made of parchment paper. With the use of computer-controlled CO_2 optical trimming and engraving machinery, the texture of the parchment paper was altered. The parchment sheet was treated after being spread open and placed on a pedestal. The intended pattern was created on the parchment paper using rapid scanning of the laser beam

throughout the face. However, its usage is constrained by the need for expensive equipment and cautious processing.

2.1.6 Plotting

In the earlier days, 2D plotter was used for the fabrication of PADs. It is a charting tool that can print or plot two-dimensional items on a plane. By altering the type of plotter head being used, one can switch between plotting and printing [25]. Fabrication of PADs often involves the employment of a spray nozzle that emits an ink stream. A 2D plotter sprays hydrophobic ink onto the paper that is within the plotter. Computing systems have the ability to predetermine or regulate the spray pattern. Depending on the density of the ink and its ability to penetrate into the paper at different temperatures, heating the paper after plotting may or may not be necessary. Bruzewicz et al. [26] modified the x-y plotter to print the solution of polydimethylsiloxane (PDMS) in hexane over the filter paper. The hydrophobic polymer entered the paper's depths and blocked aqueous solutions from entering the filter paper. This process produces inexpensive, paper-based, physically flexible gadgets. An easier approach to creating paper devices was the use of wax pens [10]. Wax was used to trace the necessary patterns across both faces of a piece of filter paper, which was then baked for a brief length of time. Because of the high temperature, the wax may melt and permeate the paper in the precise pattern of channels needed to create a hydrophobic wall. Laser plotting is another plotting technique to create microchannels by using a laser plotter [27]. In essence, the thermal deterioration action that engraves the surface of the chosen material is the basis for the microstructures produced by this technique. Ink plotting is also a commonly used plotting method in which hydrophobic barriers are created on paper using an X-Y plotter and hydrophobic inks are put into pens [26, 28]. The hydrophobic ink is absorbed in the sheet of paper due to the proper selection of ink viscosity and plotter head pressure. Although this method is cheap, the resolution of the pattern is only moderate. The method takes a long time, thus it's better suited for creating small quantities of devices.

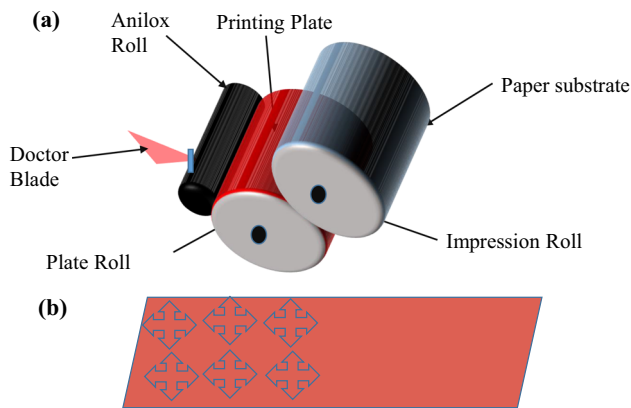


Fig. 7 Schematic diagram illustrating **a** flexographic printing method **b** structures created on porous substrate using flexographic printing

2.1.7 Flexographic printing

It is a direct and quick manufacturing technique for mass production in a roll-to-roll method as shown in Fig. 7 [9, 29]. On various substrates, commercial flexographic printers can manufacture the devices at very high speeds. An anilox roll is charged with ink, which is then delivered to a paper that is fastened to the impression roll. As an ink, polystyrene solution in an organic solvent is employed at various concentrations. The amount of ink transferred from the anilox roll to the printing plate, which has a design known as the relief pattern, is determined by the numerous cells that surround it. The doctor's blade removes any extra ink that may still be present in the anilox roll. To distribute the ink to the paper, the anilox roll is turned four times, along with the plate roll and impression roll. Getting enough ink to saturate the paper substrate, the optimization of the printing speed and pressure between rolls is necessary. The pipet is configured to automatically add ink to the ink tank after printing the first layer. After finishing a few ink layers, the anilox roll needs to be washed; otherwise, the print quality begins to deteriorate. The hydrophobic characteristics of the printed layers are influenced by the number of layers that are printed. Flexographic printing is used to print channels through the use of polystyrene ink that had been dissolved in volatile organic solvents. By adjusting the solvent's viscosity, vapor pressure, and polystyrene content, channels on the device can be printed partially or entirely through the paper. Flexographic printing also uses commercial ink PDMS. For PDMS to cut through paper, multiple replicate print layers are needed.

2.1.8 Ink stamping

Due to the simplicity of the stamping method, it has been extensively used by researchers to create PADs using various stamps and inks [30]. The portable stamp used in the stamping method is the only tool utilized

to form a pattern on the filter paper, thus it should be simple to make and apply. A PDMS stamp is used to define a fluidic structure by bringing indelible ink into contact with filter paper. Without using any external force, the PDMS stamp was repeatedly dipped into the stone pad that had been wet with permanent ink. This allowed the stamp to make brief contact with the filter paper. Although ink stamping was straightforward and less expensive, the PDMS stamp was made in a very sophisticated manner. The filter paper was dipped into the liquid paraffin, let to cool, and then placed on the surface of the original paper. The hydrophobic barriers were created by transferring the wax from the p-paper to the n-paper using a warmed metal stamp. Since they are quick and inexpensive prototyping methods based on producing ink channels on substrate with a PDMS mark and permanent inks, the double side printing technique developed by Akyazi et al. [31] and the ink stamping method suggested by Curto et al. [32] have recently emerged as alternatives to conventional wax printing. They might be viewed as low-cost fabrication techniques, but their fundamental flaw is that because they involve manual labor, there is little consistency from one device to the next. De et al. [30] developed a new method for stamping that uses paraffin over a substrate made of chemically altered paper with the help of lightweight, portable stainless-steel stamp for quick prototyping of paper-based devices.

2.1.9 Screen printing

In this procedure, photolithography is used to pattern the desired design on a screen. The model is constructed first, and then solid wax is applied to the filter paper by rubbing it through a screen model. The wax was heated after printing so that melted wax could seep into the substrate and create hydrophobic barriers using a heated plate. Sameenoi et al. [33] applied polystyrene rather than wax onto the paper in a screen printing model. This method is appropriate for modest amounts of PAD manufacturing because screen printing is frequently utilized in the production of pieces of printing materials. This method has the benefit of being compatible with a greater variety of inks. The key drawback is that it is not suited for quick device prototyping because of the high number of screens needed.

2.1.10 Plasma treatment

Plasma treatment was utilized to construct μ PAD by initially making a hydrophobic surface, and then hydrophobic material was then precisely removed by presenting the substrate to plasma over a physical barrier with the necessary pattern. The shield stay helps in the selective etching of the porous substrate and makes the paper sheet a combination of hydrophobic and hydrophilic regions. Alkyl ketene dimer(AKD) and octadecyltrichlorosilane (OTS) are two chemicals that are frequently used to make paper hydrophobic. Both

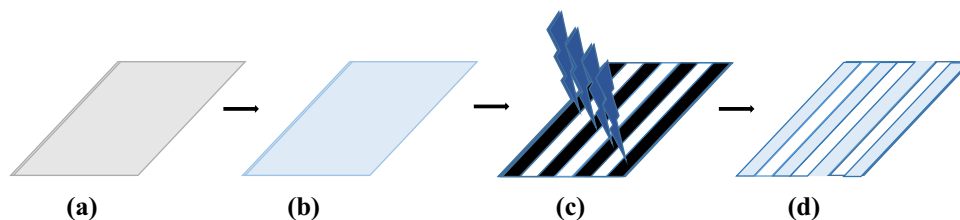


Fig. 8 Schematic illustration of designing of μ PADs: **a** paper, **b** octadecyltrichlorosilane (OTS) coated paper, **c** soft pad and PMMA mask were separated by OTS-coated paper and subjected to corona discharge after assembly, **d** patterned μ PAD

a plasma cleaner [34, 35] and a portable corona generator [36] have been proposed for plasma treatment. Li et al. [34] patterned the paper by dipping it in an AKD–heptane solution and then putting it in a fume hood evaporate the heptane. The AKD was then treated on filter paper by heating it in an oven, making the material hydrophobic. A vacuum plasma reactor was used to process the modified paper while it was positioned between two metal masks with the necessary patterns. Following the plasma treatment, the exposed portions turned hydrophilic. As a typical industrial material, AKD is affordable and easily accessible. However, each pattern is unique to metal masks. The metal masks should be costly and difficult as a result. Fluorocarbon plasma polymerization for the creation of PADs was proven [37]. Two masks i.e., a positive mask and a negative mask were tightly positioned on either side of the filter paper. Afterward, the plasma system made the hydrophobic barrier on sandwiched by puncturing the fluorocarbon. Obeso and colleagues have reported using plasma and poly (hydroxybutyrate) for the production of PADs. The plasma procedure resembles the plasma therapy that was previously mentioned. But in this instance, the paper is dried at ambient temperature after being submerged in various solutions in succession. This method involves producing the paper beforehand, which takes time but results in a straightforward plasma procedure.

2.1.11 Chemical vapor-phase deposition

Kwong and Gupta [38] first introduced the chemical vapor-phase deposition-based patterning technology for functional polymers, and afterward, the methodology was expanded for pure polymers. A magnet and a metal mask were positioned on either side of the filter paper. The monomer was placed in a sublimation chamber that had been emptied in order to undergo pyrolysis and create radical monomers. These were applied to the exposed area of the paper, where they were subsequently polymerized to form hydrophobic barriers. Then, a similar method for creating PADs that involved vapor-phase layering of pure polymers was published [39]. In the latter procedure, a magnet and a metal mask were placed on top of the filter paper. A suitable quantity of monomers was added to an evacuated sublimation chamber, where they were allowed to evaporate before being pyrolyzed into radical monomers.

They were then applied to the exposed surface of the paper and polymerized to form hydrophobic barriers. This technique was also employed to create PADs. The only distinction between the two techniques is the polymer that Chen et al. [40] utilized, a fluoropolymer covering of poly (1 H, 2 H, 2 H-per-fluorodecyl acrylate).

2.1.12 Hand-held corona treatment

Jiang et al. [41] proposed the fabrication of μ PAD using corona discharge and created PADs using a portable corona treater. First, octadecyltrichlorosilane (OTS) was used to make a filter paper hydrophobic as shown in 8. After that, a plastic mask was used to expose the hydrophobic paper to the corona. The portion that was exposed changed from being hydrophobic to being hydrophilic as a result.

2.1.13 Fast lithographic activation of sheets (FLASH)

FLASH is based on photolithography in which UV light and a hotplate are the essential tools required for it [8]. In contrast to photolithography, FLASH does not require a clean space. If UV lamp and hotplate are not accessible, FLASH method can still be successfully used in the sunshine. This technique makes it simple to design in paper small hydrophilic channels as small as 200 μ m. Photomasks are created as previously described. The photoresist is poured onto the paper and distributed evenly during the FLASH process as shown in Fig. 9. In order to evaporate the propylene glycol monomethyl ether acetate (PGMEA) included in the photoresist. During the cooling process, the paper is brought to ambient conditions. A transparency film is applied to one side of the paper, and black construction paper is applied to the other, in order to reduce the reflection of UV radiation. The border of the construction paper should have adhered to transparent film with the three parts. On the transparent film, black patterns were imprinted to distinguish between hydrophilic and hydrophobic regions. Now, a brief UV exposure is given to the FLASH material. The transparency film and construction paper are then taken off. The paper is cleaned with isopropyl alcohol and acetone after soaking in acetone for one minute.

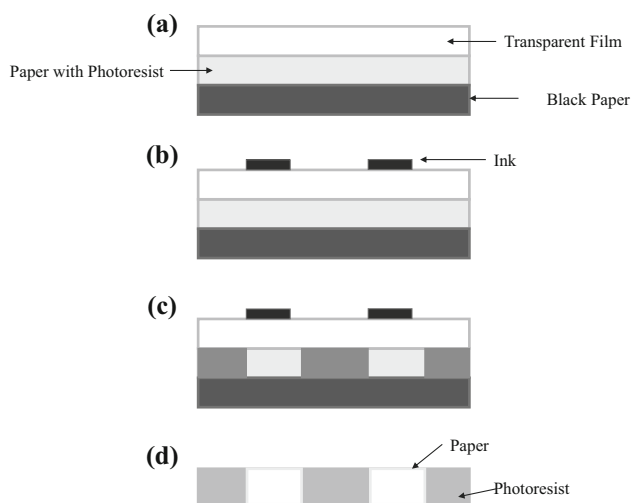


Fig. 9 Schematic diagram for FLASH method to fabricate microfluidic device **a** after applying the photoresist to a paper, sandwich a black paper between an adhesive transparent material, **b** utilising an inkjet printer to print designs onto substrate, **c** the paper being exposed to UV light, **d** peel out the transparent film and black paper from the impregnated paper

2.1.14 PDMS screen printing

On chromatography paper, hydrophobic barriers are made using the polymer PDMS, which has a very flexible character. This approach involves moving substrates in different directions under the control of a printing table. The chromatography paper is covered with a nylon mesh screen stencil that has been designed according to specifications. After that, PDMS is applied to the surface and rubbed into the chromatography paper to create a pattern over the paper. The patterned paper is dried for 30 min at 120 °C before being chilled to room temperature, as depicted in Fig. 10.

The comparison of different patterning techniques highlighting their principles, benefits, and drawbacks are mentioned in Table 1.

2.2 Incorporating operational functionality

Although paper is a unique substrate for containing liquids in specific areas and controlling fluid flow without the use of external power, the above characteristics of porous substrates only provide a limited amount of control over fluid transport, particularly over flow rate and direction. These limitations render inappropriate handling of complex chemical matrices and ill-timed performance of multi-step tasks. The early PADs had limited influence in the analytical community because they were incapable of performing complicated tasks. To integrate enhanced capability for handling liquids and enabling safe operation, various functionalities were incorporated into the device.

2.2.1 Flow rate control (programming and timing)

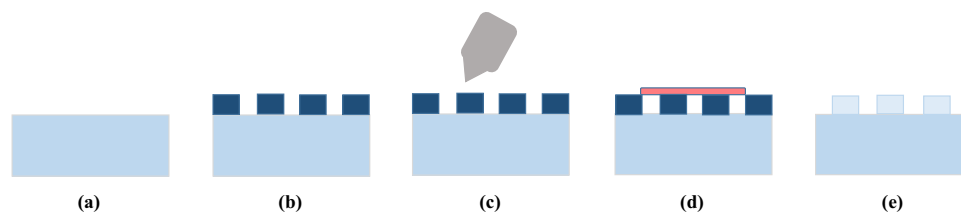
One of the earliest examples of fluid flow control was made by Martinez et al. [42] in 2010, who created a multi-dimensional μ PAD with ‘on’ buttons that could be used only once to change the flow path. When pressed, fluidic channels were connected between layers of porous material and tape that were strategically spaced apart. Until it was pressed, this computerized valve could fully stop the flow. While single-use valves have their drawbacks, this work showed how programmable PADs might be useful for testing or manually regulating the sequence of reactions. Other researchers [43–45] published additional techniques for managing fluidic transport by changing the shape of the channel. When a channel junction changes from narrow to wide, the flow rate decreases. Another way of flow control was introduced by Toley et al. [46] by redirecting the flow through an adjustable cellulosic shunt that was put in the direction of flow and in direct contact with the paper. By wicking fluid via a bridge made of soluble sugars, Houghtaling et al. [47] used a similar idea to digital ‘on/off’ switches, successfully shutting off the flow. Afterward, a water-soluble pullulan film was created by Jahanshahi et al. [48] that performed a comparable function.

2.2.2 Multi-step processing

Automating multi-step procedures is the first step in the trend toward making PAD tests more functional. By adding numerous steady portions of paper for each step of the reagent addition process, Fu et al. [49] and Lutz et al. [50] examined the successive transportation of various chemicals to a detecting zone. To build an automated sandwich ELISA experiment, Apilux et al. [51] defined numerous flow routes of variable lengths with various chemicals in each path. Li et al. [52] use of magnetically timed ‘open/closed’ single-use valves allowed them to show device control for multi-step tests. The facial tissue that made up each valve was essentially a porous substance attached with a cantilever. At the beginning of time, either the valve was lowered onto the stream, allowing fluid to flow through it, or it was lifted just above stream, preventing flow. The cantilever was activated by a resistor when the stream from the inlet approached the resistor. The intended delay for on-chip processes determined the length of the timing channel. Furthermore, Fridley et al. [53] showed that depending on the manner in which reagents are put in devices, compounds dried in the paper are amenable for multi-step processing. In their method, a single detection zone made by a PAD cut from nitrocellulose was downstream of channels that carried dry chemicals and each was a different size from the monitoring zone. All three reagents in the porous substance attached at the same time and were closest to the detection zone overall arrived and reached the detection zone first. In an effort

Table 1 Different fabrication techniques and their underlying principles, along with benefits and drawbacks

Method	Patterning Agent	Patterning principle	Benefits	Drawbacks
Photolithography	Photoresist	Physical blockage of paper pores	Good resolution, convenient, narrow width channels	Expensive agent and equipment, extra cleaning required
Wax Patterning	Wax	Physical blockage of paper pores	Mass production, simple and quick	High printer cost, poor resolution
Wax dipping	Wax	Physical blockage of paper pores	Mass production, simple and quick	Heating required
Inkjet printing	AKD	Chemical surface modification	Agent is cheap, mass production	Sophisticated steps, requirement of advanced printer
Laser treatment	Depend on paper types	Physical blockage of paper pores	Good resolution	Require extra steps
Plotting	PDMS	Physical blockage of paper pores	Cheap agent, easy fabrication, flexible	can't use for mass production
Flexographic Printing	Polystyrene	Physical blockage of paper pores	Mass production, no heat treatment	Polystyrene solution must be printed twice, and various printing plates are needed
Plasma Treatment	AKD	Chemical surface modification	Inexpensive agent, very flexible, no heat treatment required	Customized masks are required, slow production rate
Screen Printing	Wax	Physical blockage of paper pores	Easy process	Low resolution
Chemical Vapor-Phase Deposition	Chemical monomer	Chemical surface modification	High resolution	Expensive
FLASH	Photoresist	Physical blockage of paper pores	Quick	Expensive, multiple steps
PDMS screen printing	PDMS	Physical blockage of paper pores	Enhanced flexibility	Low resolution

**Fig. 10** Schematic depiction of PDMS-screen-printing method. **a** Chromatography paper **b** placing the screen on the paper; **c, d** applying PDMS to the screen; **e** curing the PDMS-Screenprinted paper in an oven

to cut the price and size of the LFAs development process, Anderson et al. [54] offered a revolutionary platform centered on the adaptability and capacity of an autonomous fluid handling system. The technology was first successfully used to create an LFA for malaria, but it was quickly expanded to allow for the development of LFAs for SARS-CoV-2 and Mycobacterium tuberculosis as well. This automatic system increased both the number and quality of LFA assay development efforts by cutting down on hands-on time, increasing experiment size, and facilitating enhanced repeatability.

Another automatic flow shutdown system was created using pullulan, a quickly dissolving polymer [48]. The paper channel is partially replaced by a deflectable capillary channel produced by a dissolvable film, enabling automatic flow control. In order to accommodate time-sensitive or multi-step reactions and tests, the user can manage fluid movement using this time-dependent flow shutdown technology.

2.2.3 Switches and valves

Device construction must enable effective control over fluid motion and multi-step protocols. A switch was achieved in PAD by manually bifurcating the channel in order to allow or prevent the capillary flow [34]. The valves operate on the idea that exerting pressure on two vertical fluidic channels changes their gap, allowing fluids to wick along the connected channels. However, functioning without controller or actuator, valves are challenging to integrate into paper-based devices. Switches and valves were built on the same platform and were utilized for more specific applications. The idea behind paper-based microfluidic valves is comparable to that of electronic field programmable gate arrays. Likewise, Martinez et al. [42] built a valve mechanism in 3-D μ PADs by exerting pressure to close the space between two fluidic channels that were vertically aligned. Fluids can wick along the joined channels by sealing the gap. Then, Glavan et al. [55] and Liu et al. [56] implemented the folding valve concept into an open-channel device and a laminated device, respectively. When channels in folding valves are folded and unfolded, the direction of fluid flow changes; folding the channel past a 90-degree angle stops the flow. In the literature, self-actuated type valves were also mentioned for sample in/ out tests. Newsham et al. [57] examined and modeled multiple configurations of thermally actuated valves to incorporate the valve into an LFIA with exact control over various flow parameters. To specifically characterize the microfluidic properties of PAD, fluorescent nanoparticles were measured using micro-particle image velocimetry. This method identified divergent bulk flow parameters that might explain extra variability in LFIA signal generation. Li et al. [58] demonstrated a self-powered rotating paper-based microfluidic chip with an integrated movable valve to detect thrombin. The sandwich was created by joining the DNA sequence (DNA1) and a DNA sequence ((*GOx*)-DNA2 modified by the glucose oxidase enzyme in order to get the supercapacitor signal. The (*GOx*)-DNA2 may then be released and employed to catalyse the oxidation of glucose as thrombin binds with its specific aptamer through strong binding affinity. The required voltage may be generated to refill the paper supercapacitor as a result of the (*GOx*)-triggered reaction, and a multimeter can monitor its signal.

2.2.4 Electrode incorporation

The challenge associated with paper-based devices is obtaining low limit of detection with reasonable efficiency due to a dependency on color identification of the human. Electrochemical detection ability of paper devices bridges the gap between conventional paper-based devices and advanced automatic devices. Devices based on electrochemical detection provide great sensitivity and selectivity while also being a good match for low-cost detection. Making a paper-based device compatible with commercial readers like glucometers was a

goal of the development process. The most significant factors affecting the performance of an electrochemical device are the electrode's shape, material composition, and fabrication techniques. Furthermore, various electrode materials are discussed below.

Carbon electrodes

Due to ease of manufacturing, ease of chemical alteration, and large possible opening in liquids, carbon is a desirable electrode material. For these reasons, carbon was the first material to be used as a functioning electrode in ePADs [59]. Since then, other instances of carbon electrodes and related fabrication techniques have been demonstrated. The dual-based lab-on-paper device created by Apilux et al. [60] demonstrated a quick and easy way to quantify Au(III) using colorimetry as indicated in Fig. 11.

1. Screen-printing

It is widely used method for fabricating carbon electrodes [61–64]. Polymerizing photoreactive polymer-coated screens around masks is commonly accomplished through photolithography. Another technique involves printing through a silk screen-adhered solid film with a craft- or laser-cut pattern. For the electrocatalytic detection of thiols, Dossi et al. printed an electrode that was combined with cobalt phthalocyanine [65]. Graphene or nanoparticles have also been used in other examples to increase the performance of screen-printed carbon electrodes (SPCE) [66].

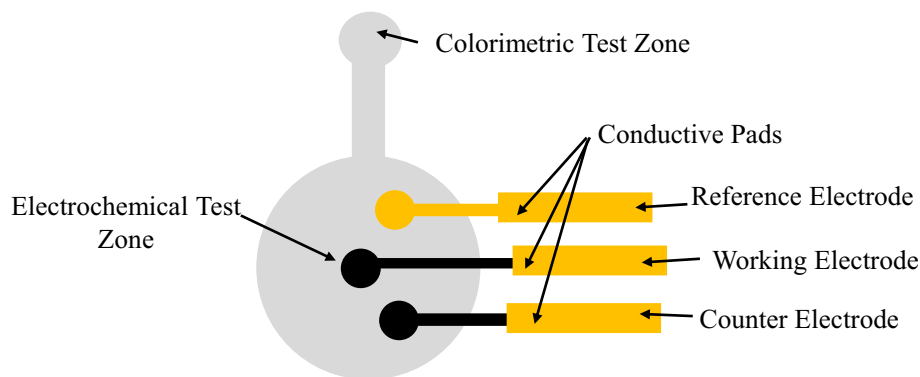
2. Stencil-printing

Screen printing and stencil printing are relatively similar processes [67]. This technique uses transparency film or sticky tape to make masks instead of the usual screen materials. Using craft or laser cutters, stencils are easily made. In order to maintain pattern fidelity while stencil printing as compared to screen printing, more dense ink is required so the electrode material is dispensed via an open hole as opposed to a mesh. Viscous ink improves electrode conductivity but reduces the endurance of the electrodes and the adhesion of the paper [68, 69]. The improvement of ink viscosity and composition can help either screen printing or stencil printing.

3. Pencil drawing

For inexpensive aqueous and nonaqueous media detection, graphite pencil leads are also used to make electrodes on paper. Santiago et al. reported using the graphite pencil concept to create electrodes for a paper-based device [70]. For precise detection, lead and graphite were first polished before being put in touch with the paper device. In early works, H-type pencils were used to create the electrodes in order to get a satisfactory electrochemical reaction. However, more recent studies have discovered that soft lead, which has a greater graphite-to-binder ratio, is the ideal material for creating conductive electrodes on paper. Dossi et al. [71] established the concept of pencil lead production after recognizing the significance of binders composition in electrodes. Different binder compositions and additives, such as decamethylferrocene or CoPC, were used

Fig. 11 Depiction of the basic design containing three electrodes (working electrode (WE), counter electrode (CE), and silver/silver chloride ink as the reference electrode (RE)) screened on patterned paper



during the pencil lead's fabrication to enhance performance and serve as a mediator during electrochemical detection, respectively.

4. Painting carbon electrodes

Painting carbon ink on electrodes directly, without using masks, is one direct way of electrode production. On apply a handmade CNT ink to the substrate and then slice it into strips, all you need is a paintbrush. To create a potentiometric sensor electrode for the measurement of potassium, ammonium, and pH, an ion-selective membrane is applied to the strips. Utilizing precut sheets of paper to outline the painting area results in more repeatable electrode geometries [72]. The mixture of carbon black and readily available carbon inks made up the ink.

Metallic electrodes

Based on either electrode modification procedures or innate electron transport processes, metallic electrodes provide a wide range of choices for electrochemical detection. The most widely utilized techniques for creating metallic electrodes are thin-layer deposition by sputtering and evaporation.

1. Thin films

It is an indirect technique for making electrodes in which metal is placed on paper after a mask has been used. By depositing metals onto the paper using sputtering, evaporation, or spraying, the paper gains conductive characteristics. Sputtering was used to deposit gold on polyester to form a metallic electrode. This electrode was used to quantify the discharge and separation of an ascorbic acid and uric acid mixture specimen on paper at clinically significant concentrations using amperometry. Then, using a metal mask and a gold-sputtered technique, 200 nm thin film electrodes were made in order to identify paracetamol and 4-aminophenol from a particular test [73]. Sputter coating is used to create platinum electrodes, which are subsequently adhered to solid substrates and put in close proximity to the paper. The flow injection detection of glucose in urine was carried out using sputtered electrodes. In urine samples, hydrogen peroxide was discovered amperometrically as a result of the reaction between glucose and glucose oxidase.

2. Wires

Compared to electrodes made of carbon ink, microwires are always thought to be a superior electrode choice. Microwire electrodes have a lower resistance than conventional electrodes, which improves the electrochemical response during detection. Additionally, they are simple to clean and/or adjust before incorporating into equipment like gold. Microwires were cleaned with piranha solution to enhance the electrochemical reactivity [74]. Employing thiol-based chemistry, which connected an inner monolayer with a negative terminal, the electrodes were subsequently altered to only react to positive analytes.

3. Microelectrodes

Santhiago et al. [68] created the first microelectrode for a paper-based device to carry out an operation identical to stencil printing, but instead of printing directly onto the paper, they used a laser to carve very small holes into a translucent sheet, which they then filled with carbon paste as seen in the picture. For electrochemical detection, elliptical microelectrodes were created using laser ablation. On the back of the transparency, several backfilled holes with a single electrical connection were constructed in order to carry out microelectrode array detection. With more microelectrodes in an array, the limiting current value for sigmoidal voltammetric curves rises.

4. Nanoparticle modification

A technique to alter the printed electrodes on the paper involves the deposition of nanoparticles. Nanoparticles can change a material's conductivity, modifying chemical functionality and expanding the surface area of electrodes. On SPCEs that are available for purchase, Pt nanoparticles were electrodeposited [75]. Pt boosted the measured current response at the electrode surface by catalyzing the oxidation of hydrogen peroxide. On the surface of the working electrode, gold clusters were also formed using electrodeposition. With the aid of gold-thiol chemistry, the gold enhanced the electrode's surface area and made it possible to attach capture aptamers. Au nanoparticles were placed on cellulose fibres treated with graphene to boost the accuracy and durability of the framework for DNA detection [76]. Additionally, Au nanoparticles were deposited on the fiber's surface, forming an interconnected layer

that served as the basis for a special working electrode [77]. High conductivity and electrodes with a large surface area are produced using these manufacturing techniques.

2.2.5 Connections

In order to generate power, μ PADs can use paper-based batteries; nevertheless, according to WHO guidelines, a flawless diagnostic device would operate without the use of additional batteries [78, 79]. These fluidic batteries are constructed so that the power supply is near the test, making it simpler to connect them. The fluidic battery cannot operate until the sample is placed inside the device. As a result, the sample can be utilized to power any required assay-related components in addition to conducting an assay. Due to integrated galvanic cells, fluidic batteries may provide the appropriate voltage or current. These cells can also be changed to incorporate the smallest amount of electrolytes and electrodes required for a specific procedure [80].

2.2.6 Detectors and readout

The production of an effective paper-based device requires patterning, but patterning by itself cannot produce a suitable device unless a decent detector is built into the device. The analyte should be able to be quantified by a paper-based instrument. A single analyte was first detected by a device; however, as paper-based microfluidic devices advanced, the idea of numerous monitoring areas to capture many analytes within a single device was introduced. After printing hydrophobic patterns onto the hydrophilic paper, sensing zones can be created by spotting chemicals in the monitoring areas. The main objective of creating accurate and user-friendly devices is to eliminate the need for external instrumentation. When a ‘yes/no’ response could determine therapy, quantitative or semi-quantitative detections or readouts are preferred for on-site diagnostics devices. The most popular method for non-instrumented analysis is the employment of an externally or internally placed visual color intensity comparator. The technology is now compatible with smartphones and detectors like CCD, CMOS, flatbed scanners, etc. that are reasonably affordable and simple to use with only light to moderate training. Due to a number of factors, mobile camera technology has evolved significantly in recent years. As a result, new opportunities for using PAD technology to investigate detection in various situations have arisen. The techniques for quantitative feedback described in this study include equipment-free methods, digital cameras, and mobile phone cameras.

Smartphones and digital cameras

Smartphones have created a wide range of new options for analysis in contexts with limited resources, whether by on-site analysis or distant data transmission to a single location. Information can be captured remotely and kept for subsequent transportation to a central

location because to the device’s enormous data storage capacity, eliminating the requirement to carry samples. In addition to having a digital camera and a light source, modern smartphones are also capable of doing tasks that would often be performed by costly spectrophotometers, fluorimeters, or silicon photodetectors. Smartphones have been used to identify drugs, biomarkers, explosives, dangerous metals, and bacterial and phage infections. Smartphones operate more quickly than flatbed scanners, however, because ambient light conditions change, image intensities are inconsistent. A smartphone intensity-correction app was created to address this issue, or detection could also be made by physically blocking ambient light while taking images.

Handheld devices

In the past, POC applications, which can cost over 10, 000, required bulky, benchtop instruments. Although these paper devices are effective for POC applications, they do not meet the ASSURED criteria (device must be Affordable, Sensitive, Specific, User-friendly, Rapid and robust, Equipment-free, and Deliverable) of the WHO for the medical or environmental community as mentioned in the preceding section due to their pricey integrated pieces. Therefore, the detector cost-structure system must be substantially lower. For simultaneous amperometric detection of glucose, lactate, and uric acid, a low-cost eight-channel potentiostat was developed [81]. The design of the gadget for multiple electrochemical detections at once included eight unique bespoke electrochemical wells. In a handheld potentiostat more recently, 48 channels were added [82]. A portable potentiostat that can mix samples on board, execute a variety of electrochemical assays, and wirelessly send analytical data over speech through a cellphone audio connection is made for environments with limited resources. It was intended for this data transfer to make older consumer phones compatible with their system. It has also been stated that other commercially available handheld instruments may measure water contamination electrochemically or explosively using fluorometry.

3 Detection techniques

Microfluidic devices based on paper have been proposed with several different detection techniques. These detection methods have applications in environmental testing, food pathogen detection, medical diagnostics, power generation, etc.

3.1 Colorimetric detection

It is currently one of the frequently utilized methods for detection in PADs because of the benefits of a visible interpretation, quick detection efficiency, practicality for rural field applications, simple operation, and good stability. In colorimetric detection, the analyte

solution is passively transported by capillary action to the test zone of the apparatus, where it reacts with properly positioned reagents to generate a perceptible color change. Basically, the digital/CMOS cameras, scanners, or cell phones used in PAD colorimetric detection systems are used to capture the detection zone images, which are then sent to a computer or a mobile device for processing. For colorimetry-based analysis, LFAs are the most popular PADs. Because LFAs are simple to use, biodegradable, quick, and lab-free, they are beneficial for POCT and allow for the quick sensing of biomolecules like proteins in complicated samples without prior pretreatment. The majority of commercial LFAs that rely on optical sensings, such as HIV testing, pregnancy tests, and other bios studies, have been developed using aptamer- or protein-labeled gold nanoparticle (AuNP) conjugate probes. A PAD for the identification of acetylcholinesterase activity and inhibitor screening was created by Liu and Gomez [83] based on colorimetric sensing. The fabrication of the PAD used a direct wax printing procedure in which wax was applied to the paper to form the hydrophobic barrier. Cardoso et al. [84] proposed a variety of colorimetric PADs for the measurement of numerous analytes, like whiskey, BSA, tear glucose, urea, ketone bodies, nitrite, glucose, bilirubin, etc [85, 86]. To detect Hg^{+2} ions, Meelapsom et al. [87] created an Ag nanoparticle-processed multi-layered PAD employing thick paper and an ink-jet printing technique. The Hg^{+2} ions used in the detecting procedure oxidized the Ag nanoparticles, causing them to break up into smaller particles, reducing Hg^{+2} to Hg, and the detection zone's color is changed from deep yellow to vibrant yellow. It was demonstrated that the gadget could detect particles as small as 1×10^{-3} ppm.

A PAD was created by Yamada et al. [88] to deliver the findings of chemical analysis in the manner of "text" by combining the utilization of a conventional colorimetric indicator with an inert colorant. Protein in urine has been utilized as a proof-of-concept model analytical target. Human urine was used in user tests, and the results showed that the created device's accuracy was on a level with a conventional dipstick.

For the colorimetric detection of Hg^{+2} , Cd^{+2} , Zn^{+2} , Ni^{+2} , and Fe^{+3} ions in drinking water or effluent using chromogenic chemicals, Mujawar et al. [89] proposed a PAD for recycling waste to create low-cost analytical devices. The Fe^{+3} ions were determined using an extremely reactive 2-hydroxy-1-naphthaldehyde (HyNA) reagent in an optical assay plate with conical wells. An excellent limit of detection and limit of quantification of total Fe^{+3} ions were achieved. The proposed approach proved successful in detecting and precisely determining Fe^{+3} ions in tap and marine water samples. Chowdury et al. [90] proposed a μ PAD added with a nanosensor made of gold and functionalized with α -lipoic acid and thioguanine for detection of arsenic in hand tubewells water. By raising the pH of the PADs to 12.1, a technique was created to prevent the influence of the alkaline metals (Ca, Mg, K, and Na) prevalent in Bangladesh groundwater.

This test, which evaluates if the concentration of arsenic in the water is beyond or under the WHO recommended limit of 10 g/L, was the inaugural paper-based test to be approved using water samples from Bangladesh. Liu et al. [91] demonstrated an effective framework consisting of a paper-based/PMMA chip with a colorimetric sensor to measure SO_2 concentrations. The sample in the suggested apparatus was kept on a small piece of paper that had been treated with an acid–base marker before being placed inside a PMMA microchip. It was shown that the SO_2 percentage results taken for 15 industrial food samples using the suggested methodology deviated from the values obtained using a recognized macroscale approach by a maximum of 4.29 percent [92]. Mahmoudi et al. [93] designed a colorimetric PAD for rapid and hands-free telomerase activity sensing by utilizing color shift in accordance with enzyme activity. The telomerase was extended along with a biotinylated probe and an oligonucleotide that was complementary to the telomeres. The hydroxylamine hydrochloride approach for enlarging the AuNPs allows for a signal enhancement that results in color that is apparent to the naked eye once the assembly has been joined. With a measurement range of 6 to 25,000 cells, visual telomerase activity identification was achieved down to 6 cells when the analytical performance of the enzyme extracted from breast cancer cells was assessed. The hue of the porous sheet evolved from light-red to light-red-blue to black-red with increasing telomerase content. Fu et al. [94] suggested a colorimetric assay for telomerase activity detection on functionalized cellulose paper using methylene blue (MB) as a colorimetric probe and was focused on telomeric elongation and collecting amplification. The telomerase substrate was placed onto sterile cellulose paper (TS). Telomerase will lengthen this primer, resulting in a long single DNA that will further catch more probes and raise the assay's responsiveness. When MB-labeled oligonucleotides hybridize with sDNA, the color will change. Signal strength is correlated with sDNA content and hence with telomerase activity. Oligonucleotides are unable to hybridize with sDNA when telomerase is not present in the samples. Telomerase will stretch this primer to generate a single DNA (sDNA), which will further attract more probes and improve the sensitivity of the assay. The color will change when MB-labeled oligonucleotides hybridize with sDNA. The quantity of sDNA and thus the activity of telomerase is associated with signal strength. In samples lacking telomerase, oligonucleotides are not able to hybridise with sDNA.

3.2 Electrochemical detection

Dungchai et al. [59] merged the concept of electrochemical detection with μ PADs. The channels in chromatography paper were created using photolithography and carbon electrodes were printed using screen-printing techniques. By sensing uric acid, lactate, and glucose

in biological samples, Dungchai and coworkers further demonstrated the device's biosensory capacity. The three different electrodes in this trial are changed with lactate oxidase, glucose oxidase, and urease, respectively, by adding enzyme solution into the corresponding test region. Diabetes is a very common disease and the glucose levels of the patient must be continuously monitored in an easy way. In order to measure glucose levels, Fernando et al. [95] created an electrochemical microfluidic paper-based analysis device (PAD) that utilizes sweat and saliva as a sample. The creation of a three-electrode system uses pseudo-reference stainless steel and a working electrode that has been anodized using sodium potassium tartrate tetrahydrate. With a limit of detection of 0.058 mmol dm⁻³ and a working range of 1 to 10 mmol dm⁻³, cyclic voltammetric-based assessment of glucose using PAD achieved a linear response.

Fonseca et al. [96] gave the basic concept of making disposable ePADs by employing screen printing and inexpensive materials. All the devices were built utilizing liner paper as a base and carbon ink that was made with wood glue and graphite powder. The ePAD was assessed as a biosensor and electrochemical sensor. Moreover, Tomei et al. [97] fabricated a strip to identify the level of glutathione in blood. A filter paper was used as a substrate where WE and CE were screen-printed, hydrophobic channels were wax printed and then the solution was confined in an area to prevent diffusion of electric contacts. The loaded cystamine on WE and the glutathione, which was liberated by blood lysis, engage in a thiol-disulfide exchange reaction, which is the basis for the detection. Due to the electrocatalytic abilities of Prussian Blue included in the WE, this reaction results in cysteamine, a molecule readily oxidizable.

Ruecha et al. [98] proposed a label-free disposable PAD to detect human interferon-gamma (IFN- γ) by making three electrodes on the Whatman filter paper grade No. In order to screen print the working electrode (WE) and the reference (RE) and counter electrodes, the wax-patterned device was divided into two tabs (CE) so that they can fold over one another. The working electrode was made with graphene ink and polyaniline to immobilize human IFN- γ monoclonal antibodies covalently.

Wang et al. [99] developed an origami-style device to detect breast cancer MCF-7 cell line. Three spatially isolated sections of wax and a screen-printed WE of carbon were printed on paper grade 2. The hydrophilic zone in the reference region also has a carbon CE and an Ag/AgCl RE. The produced Au@3D-rGO was then coated with the MCF-7 cell-specific aptamer H1. To make it straightforward to combine the full screen-printed, three-electrode electrochemical cell, the different patterned pieces of the paper component were wrapped in a two-step folded pattern once the solution had been added. Likewise, Moazeni et al. [100] detected the biomarker of tumor i.e., α -fetoprotein in human serum by embedding finger-type silver-carbon electrode pairs on paper substrate. The devices were created using a top layer of a substrate treated with aldehydes

and a lower flexible sheet of plastic. Diphenylalanine nanostructures were positioned on the paper to integrate different groups and help with the covalent immobilisation of antibodies to the target compound. To detect CEA in samples of human serum, another paper employed the multilayer structure. On a section of the device with structure, a molecularly imprinted polymer (MIP), which was electro-synthesized in the presence of the target analyte, was electro-synthesized and used as the particular receptor for these target analytes. In a different but identical portion of the device, a non-imprinted polymer was created in the same way as the MIP [101]. Also, for the rapid and easy identification of infectious diseases, brought on by pathogenic microorganisms by aiding affinity-based biosensors and amplification of the genetics were used in many papers. Like, He et al. [102] created an origami style PAD to identify the salmonella pathogen *Salmonella typhimurium* by combining wax and screen printing. By flipping the various origami pieces, the device was used to execute cell lysis, DNA extraction, and LAMP. When compared to PCR results, the device could identify the pathogens in whole blood with a sensitivity of 82 percent and a specificity of 91 percent. Finding antibiotic resistance is an intriguing strategy for managing infectious diseases. Santhiago et al. [103] described the electrochemical characterization of a 3-D PAD for p-nitrophenol analysis. The filtration-integrated PAD was made using regular printing paper that had been wax-printed with a design to allow quick evaluate p-nitrophenol information with a quick response code. The instruments were used to measure the presence of p-nitrophenol in water samples, with a recovery rate varying from 91.8 to 108.2 percent. Nowadays, cardiovascular disease (CVD) is the major cause of death worldwide. As a result, for the diagnosis and monitoring of illnesses, a sophisticated and reasonably priced POC-detecting device is required. Bookaew et al. [104] made an ePAD to simultaneously measure three key CVDs biomarkers, including C-reactive protein (CRP), troponin I (cTnI), and procalcitonin, using a label-free immunoassay. The sample inlet, all detection zones, and their connecting channels were defined by wax on the paper. They used square wave voltammetry to measure the concentrations of the CVDs biomarkers (SWV). When the cardiac marker was present, there was a noticeable reduction difference in the response curve in a concentration-dependent manner, even though there was no discernible difference in the response curve when it was absent.

Yakoh et al. [105] designed two models for fluid delivery in a μ PAD that can successively store and transport reagents to the required zone without an external source. This 3D capillary-driven device was made of origami folded paper and a portable pad for electrochemical detection of biological organisms to illustrate the breadth of this technique. The single buffer injection was developed for ascorbic acid sensing utilizing a flow-through arrangement. They extended the usefulness of the device to integrate experiments by adopting a stopped-flow mode.

3.3 Fluorescent detection

It is centered on the estimation of the amount of light that a material emits after having first absorbed electromagnetic radiation. It typically encounters problems in PADs because a commonly available paper with chemicals that also self-fluoresce and generate a lot of background noise. However, numerous fluorescence sensors incorporated with any textile material have been created and have poor sensitivity. Wang et al. [106] illustrated a cloth/paper hybrid μ PAD for identification of mercury (Hg^{+2}) and lead (Pb^{+2}) ions in water. After adhering quantum dots to the cotton cloth, ion-imprinted polymers were employed to alter the fluorescence-detecting cloth-based component (IIP). The limits of detection for the fluorescence signals were achieved using fluorescence quenching action. Zhu et al. [107] tested Alkaline phosphatase and butyrylcholinesterase simultaneously by 3D origami μ PAD in which sample-in-result-out platform fitted. These two indicators were also used in a rationally designed cascade catalytic reaction for sensing ALP and BChE. Using appropriate metal molds and one-step mapping with a black oil-based pigment, a 3D origami PAD with 4 levels and two parallel channels was created. Using a smartphone camera and red-green-blue software, fluorescent images on the detecting region can be obtained after simply folding the paper and then again unfolding nearby surfaces to begin the reactivity of charged chemicals. Under ideal circumstances, the suggested platform was used to sense ALP and BChE in human serum samples do not necessitate any preparatory procedures. Shi et al. [108] proposed a simple method for creating carbon nanodots that are nitrogen-doped in yellow fluorescence (y-CDs). The 4-amino salicylic acid was used as the precursor compound in a one-step hydrothermal process without further surface passivation or modification to create the sensor strip of paper comprising y-CDs. These y-CDs have been used for intracellular Al^{+3} imaging and paper-based Al^{+3} sensing in living cells without interference from autofluorescence because of these outstanding features. In order to detect Hg^{+2} ions, Zong et al. [109] created the reversible red fluorescent probe the (NDI-5), which was primarily composed of the receptor bis[2-(3,5-dimethylpyrazol-1 yl)ethyl]amine and the strong electron-withdrawing unit naphthalene diimide. The probe NDI-5 showed a rapid and selective ‘turn-on’ fluorescence response to Hg^{+2} ions because the coordination of Hg^{+2} ions can push the potential twisted intermolecular charge transfer (TICT) in the entire molecule. For the semi-quantitative testing of Cu^{+2} ions, Liu et al. [110] showed how to make dual-colored CD ratiometric fluorescent test paper. The visual assessment of Cu^{+2} ions using the ratiometric fluorescent test paper has been effectively created in multiple key areas. (1) The remaining p-PDA effectively binds Cu^{+2} ions on the surface of r-CDs. (2) The Cu^{+2} ion functions as a link, allowing the small b-CDs to be transferred onto the surface of larger r-CDs by its double coordinating connections with the surface ligands of both r-CDs and

b-CDs. (3) The b-CDs undergo a particular spectral energy transfer to the r-CD- Cu^{+2} complex.

3.4 Chemiluminescence detection

Another sensitive and effective detection method for PADs is chemiluminescence sensing. The method shines in terms of its ease of use, fast response, and interoperability with micro technologies, enabling numerous applications, even for those who are not trained [111]. However, the sensing must be done in the dark, which makes it more difficult to make the device. Portable chemiluminescence readers are also required for this procedure. The chemiluminescence (CL) technique and μ PADs were integrated for the first time by Yu et al. [112] to create a unique CL PAD biosensor. The oxidase enzyme reactions and the chemiluminescence reaction between a rhodanine derivative and produced H_2O_2 in an acid medium are the foundations of this lab-on-paper biosensor. This CL PAD biosensor was skillful in quantitatively determining uric acid with accurate and satisfying results. Then, the same researcher [113] created a PCAD to sense both glucose and uric acid in fake urine simultaneously. They discovered that by varying the ranges that the samples traveled, it was feasible to simultaneously measure uric acid and glucose. Al et al. [114] invented a portable PAD for on-site screening of dangerous mercury ions (Hg^{+2}) in cosmetics with a limit of detection of 0.04 g ml. It is founded on the fundamental ability of quantum dots of carbon (CQDs) to function as an excellent emitter for the bis(2,4,6-trichlorophenyl)oxalate (TCPO)-hydrogen peroxide (H_2O_2) CL reaction. Zangheri et al. [115] created a biosensor that uses a CL-lateral flow immunoassay (LFIA) technique to detect salivary cortisol quantitatively using a smartphone app. The biosensor works by using a peroxidase-cortisol conjugate in a direct competitive immunoassay and detecting the result by incorporating the chemiluminescent substrates enhancer/ H_2O_2 /luminol. It provides quantitative analysis between 0.3 and 60 ng/ml for the therapeutically appropriate range of salivary cortisol detection.

3.5 Electrochemiluminescence

Electrochemical processes are the basis for electrochemiluminescence sensing methods, which produce luminescence. When electrochemically produced intermediates go through exergonic processes, they enter an electrically excited state. As they unwind and become more tranquil, the molecules in this condition produce light, enabling monitoring systems without a photodetector being necessary. The ability of electrochemiluminescence sense to be enforced to both luminescence and electrochemical sensing techniques is its most notable characteristic. In comparison to chemiluminescence, electrochemiluminescence also has some benefits, including a decreased background, the ability to manage reagent synthesis, and greater selectivity through

potential control [116]. Delaney et al. [117] firstly merged paper microfluidics with electrochemiluminescent (ECL) detection by paring inkjet-printed paper with screen-printed electrodes, that may be read without a conventional photodetector. For the first time, Wu et al. [118] created a paper-based electrochemiluminescence (ECL) origami device (PECLOD) and combined the rolling circle amplification (RCA) method with oligonucleotide functionalized carbon dots (CDs) to create a cascade signal amplification method for the sensing of IgG antigen. The RCA product's tandem-repeat cycles could serve as an excellent model for the regular construction of CDs, which would then display many CD tags for ECL readout per protein recognition event. The recently suggested wax-printed 2D μ PADs based on immediately screen-printed electrodes on paper was the first to incorporate electrochemiluminescence (ECL) immunoassay [119]. Four tumor markers were identified using a standard tris-(bipyridine)-ruthenium-tri-n-propylamine ECL system in actual clinical serum samples. Eight working electrodes were consecutively inserted into the circuit with the help of a simple mounted and a section switch included into the analyzer to start the ECL response in the scanning band between 0.5 to 1.1 V at ambient conditions. Yan et al. [120] included electrochemiluminescence immunoassay capabilities into wax-patterned PADs that were based on screen-printed electrodes. At room temperature, the ECL reaction was started with the help of a homemade device holder. This paper-based ECL 3D immunodevice was utilized to perform a standard tris(bipyridine)ruthenium-tri-n-propylamine ECL system for the diagnosis of carcinoembryonic antigens in actual clinical serum samples.

4 Theoretical Analysis

The fluid moves in the porous substrate can be categorized into two processes, the wet-out process, and the fully wetted flow (as shown in Fig. 12). The wet-out process: the fluid is moving forward the dry porous media. It is modeled using the Lucas-Washburn equation. In the fully wetted flow, the fluid moves along the wetted porous media and is described by Darcy's law.

4.1 Lucas-Washburn equation

Lucas and Washburn proposed this model to explain the behavior of liquid wicking in porous materials. The porous microstructure of paper can be compared to a collection of cylindrical tubes where capillary action drives the liquid flow [121]. It is a process of momentum balancing between the hydrostatic pressure, capillary force, and viscous force.

According to L-W equation: Inertia force = surface tension + gravity force + viscous force

$$\rho\pi r^2 \frac{\delta}{\delta t} \left(h(t) \frac{\delta h(t)}{\delta t} \right) = 2\pi r \sigma \cos \phi - \pi r^2 \rho g h(t) - 8\pi \eta h(t) \frac{\delta h(t)}{\delta t} \quad (1)$$

where σ is surface tension, r is the radius of the meniscus, ρ is the density of the liquid, ϕ is the equilibrium contact angle and h are distance the liquid front has traveled. The Lucas-Washburn model considers a few key assumptions, including that (i) evaporation does not take place (ii) gravity and inertia forces are neglected, (iii) the fibrous porous material is homogeneous, (iv) boundaries have no impact on capillary flow, and (v) wicking liquid is laminar, incompressible, and low viscous. In consideration of these assumptions, Eq. (1) will become,

$$2\pi r \sigma \cos \phi = 8\pi \eta h(t) \frac{\delta h(t)}{\delta t} \\ h = \sqrt{\frac{4\sigma \cos \phi \zeta}{\eta \epsilon r}} t^{1/2} \quad (2)$$

Where t is the liquid absorption period and h is the length of the paper's wetted area after time. Since σ , ϕ , η , and r are all constants and the wicking length (h) is proportional to the square root of time the fluid-front velocity drops over time due to the flow resistance provided by porous media's surface [49]. The aforementioned assumptions place restrictions on Eq. (2). As a result, many changed models are created to provide better explanations.

4.1.1 L- W model considering gravity force

In some circumstances, it can be challenging to utilize the standard L-W equation to determine the performance of device as different diagnostic tools and experimental paper strips operated vertically. The force of gravity commences existing as a result of fluid flowing vertically. The gravitational force eventually becomes a significant role in the liquid immigration process as the liquid rises, which causes a substantial difference between the theoretical and experimental liquid front. A general correlation between the liquid front and time is created to address this issue [122, 123].

From Eq. (1) we obtain

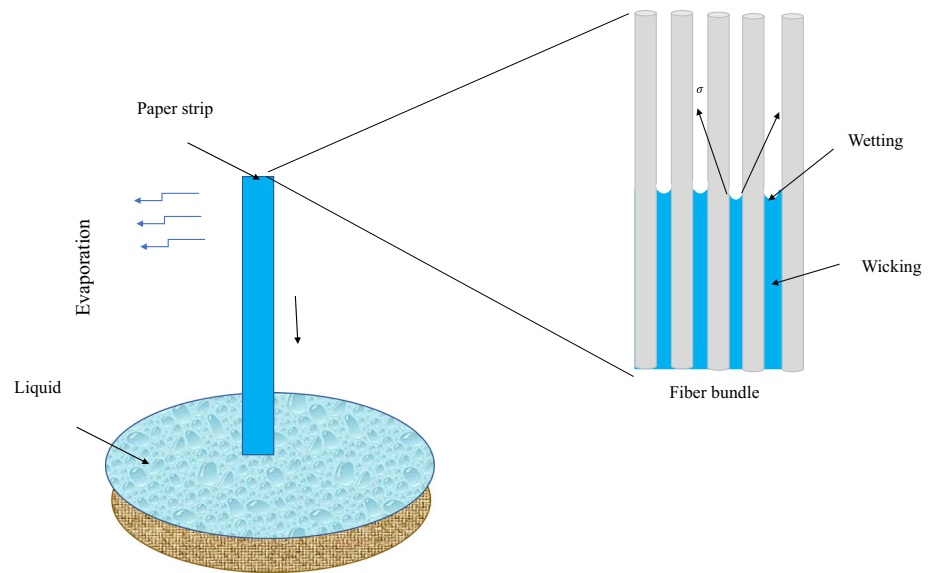
$$2\pi r \sigma \cos \phi = \pi r^2 \rho g h(t) + 8\pi \eta h(t) \frac{\delta h(t)}{\delta t}$$

The equation can be further written in the scaling form:

$$\frac{\sigma}{rh} \sim \rho g + \frac{\eta h}{r^2}$$

Therefore, the driving capillary pressure gradient is balanced by both the force of gravity and viscous friction.

Fig. 12 Representation of physical mechanisms governing the behaviour of liquids in porous materials



After integrating the above equation

$$h = \sqrt{\frac{2\sigma r t}{\eta}} - \frac{\rho g r^2 t}{\eta}$$

Substituting the radius r_l of the leading meniscus (deduced from the condition $(\frac{\delta h}{\delta r}) = 0$ at $r = r_l$) in the previous equation

$$r_l \sim \left(\frac{\eta r}{8\rho^2 g^2 t}\right)^{1/3}$$

we obtain the value of $h(t)$ at $r = r_l$

$$h(t) \sim \left(\frac{\sigma^2 t}{\eta \rho g}\right)^{1/3} \tag{3}$$

The connection demonstrates that the h has a linear relationship with $t^{1/3}$ as shown in Eq. (3).

4.1.2 The modified model considering evaporation

When the temperatures are high and the relative humidity is low, the assumption that there is no evaporation occurs may cause an overestimation of liquid flow over an extended period in an open environment. By ignoring the gravitational influence, one can examine evaporation, which is consistent with observations on the wetting process [48, 124]. Empirical correlation from the ASHRAE handbook to calculate the rate of water evaporation at each relative humidity,

$$m_{ev} = (p_s - p_p) \times \frac{(0.089 + 0.0782 h_{fg})}{m_a}$$

where, p_s, p_p, h_{fg} , and m_a are the saturation pressure, partial pressure of water vapor, latent heat of vaporization, and air flow rate respectively. The partial pressure of water vapour in the air and the water saturation pressure at a fixed pressure and temperature are used to define the relative humidity. The relative humidity

$$(\pi) = \frac{p_p}{p_s}$$

Therefore, we obtain

$$m'_{ev} = (1 - \pi) \times p_s \times \frac{(0.089 + 0.0782 \times h_{fg})}{m_a} \tag{4}$$

The integral formula can be used to determine the total evaporation mass at every instant in the evaporation model:

$$m_{ev} = 2 \int_0^t m'_{ev} w \tilde{h} dt \tag{5}$$

where, \tilde{h} is the expected wicking height of the liquid. The expected wicking liquid mass m_e at any instance is the difference between the theoretical value m_o and the evaporation mass m_{ev} ,

$$m_e = m_o - m_{ev} = \rho w \delta \sqrt{\frac{4\sigma \epsilon \cos \phi \zeta}{\eta r}} t^{1/2} - 2 \int_0^t m'_{ev} w \tilde{h} dt$$

Wicking mass of liquid m_e can be attained by the wicking liquid density and its volume,

$$m_e = \rho w \delta \epsilon \tilde{h}$$

Therefore, the wicking liquid height can be given by

$$\tilde{h} = \frac{m_{ev}}{\rho w \delta \epsilon} = \sqrt{\frac{4\sigma \cos \phi \zeta}{\eta \epsilon r}} t^{1/2} - \frac{2m'_{ev}}{\rho \delta \epsilon} \int_0^t \tilde{h} dt \quad (6)$$

By taking a time derivative, the Eq. (6) is recast as:

$$\frac{d\tilde{h}}{dt} = Rt^{-1/2} - S\tilde{h} \quad (7)$$

Boundary condition: $\tilde{h} = 0$, at $t = 0$

$$R = \frac{2m'_{ev}}{\rho \delta \epsilon}$$

$$S = \sqrt{\frac{\sigma \cos \phi \zeta}{\eta \epsilon r}}$$

The solution to Eq. (7) is therefore

$$\tilde{h} = 2Se^{-Rt} \int_0^{\sqrt{t}} e^{Rt^2} dt \quad (8)$$

The liquid-wicking process exhibits a dynamic character due to evaporation. Equation (8) represents the wicking distance with due accounting of evaporation from the surface. This adjustment may be needed depending on the particular experiment.

4.2 Darcy's Law

It was first used in 1856 to describe the fluid flow through a fully saturated porous substrate by Henry Darcy [125]. This model was created using the momentum equation to address the issue of liquid flow in pre-wet porous media under steady-state conditions. By examining how water moves through sand, the viscous pressure loss is written as:

$$\nabla P = -\frac{\eta}{\zeta} v \quad (9)$$

where v is the average velocity vector, ζ is the substrate permeability, η fluid viscosity, and ∇P is the pressure drop per unit length also known as Laplace pressure. Using the paper substrate, calculate the fluid's imbibition rate (\hat{v}), the above equation is further expanded to yield:

$$\hat{v} = \frac{\zeta_i \nabla P}{\eta h(t)}$$

where $\zeta_i = \frac{\zeta}{\epsilon}$ is the interstitial permeability and the porosity $\epsilon = 1 - \frac{\gamma}{\rho h}$, γ is the weight, ρ and h are the density and thickness of the paper respectively. Darcy's law

finds out the flow rate Q under a pressure differential ∇P , by using the Navier–Stokes equation:

$$Q = -\frac{\zeta \gamma h}{\eta L} \nabla P \Rightarrow \nabla P = -\frac{\eta L}{\zeta \gamma h} Q \quad (10)$$

In this expression, $\nabla P = P(0) - P(h)$, where $P(0)$ is the pressure at $x = 0$, and $P(h)$ is the average capillary pressure. A hydrodynamic load term with a general flow resistance R_{hyd} is also included in the flow domain for the model system under consideration

$$Q = -\frac{\nabla P}{R_{hyd}}$$

The above equation is analogous to Ohm's law of an electrical circuit, $I = \frac{\nabla V}{R}$, where I is the electric current, R is the electrical resistance and ∇V is the potential drop. In hydrodynamic systems the volumetric flow rate, Q is the volume per unit of time, while in electric system current is the charge per unit of time. Also, ∇P is analogous to potential drop.

Since capillary force is the primary factor influencing analyte transport in PADs, low spontaneous imbibition rates may reduce the detection sensitivity. For building sensitive and precise PADs, a quantitative understanding of internal spontaneous capillary flow progression is necessary. Wang et al. [126] examined the capillary flow in a porous substrate both experimentally and numerically. The authors computationally analyzed the experimental data in order to enhance the prediction of spontaneous imbibition. The quasi-static pore-network modeling of a real filter paper used to establish the equilibrium two-phase flow material parameters reveals that neither the single-phase Darcy model nor the Richards equation adequately anticipates spontaneous imbibition. A new numerical simulation using the finite element method called PORE-FLOW was presented to describe these imbibitional flows in wicks with complex forms [127]. Additionally, two-dimensional (2D) wicking in modified cylindrical wicks with two different cross-sectional areas is predicted using the simulation. Later, the wicking behavior of a few further types of changed wicks with noticeable changes in their cross-sectional areas was statistically examined. It was found that the history of the liquid ingested was related to the height of the liquid front as a function of time. The Richards equation, which accounts for the dynamic capillarity effect, shows the capacity to predict when wetting saturation will begin. Liu et al. [128] used three-width strips of filter paper to measure the liquid mass and height through experimental and numerical investigation. To calculate wicking height and mass, a modified model that takes the evaporation impact into account was developed. It was found that after initially declining sharply, the wicking speed stabilized at a lower level and remained steady. With a wider strip, more wicking mass could be achieved, but reagent loss increases in proportion.

Ouyang et al. [129] advanced the use of the numerical simulation method to examine PAD fuel cells. To show how the paper-based microfluidic fuel cell functions as a whole, both transient and steady-state modes were used. Moreover, the effects of several structural characteristics on cell performance, such as electrode spacing, the distance between the electrode and the inlet, channel thickness, and electrode length, were also explored. Results demonstrated that decreasing cell output power to varying degrees, as major structural factors are increased. Modha et al. [130] described the behavior of paper-grooved channels and evaluated how well they function as ‘delay’ mechanisms for a multi-fluid paper-based sensor. Moreover, the author also performed *In-silico* simulations that can accurately anticipate imbibition in both natural paper and grooved channels. Elizalde et al. [131] hypothetically investigated capillary imbibition in substrates that mimic paper in order to more clearly visualize fluid transport in the context of the macroscopic shape of the flow domain. A model that predicts the cross-sectional profile required for a specific fluid velocity or mass transfer rate has been created for uniform materials with arbitrary cross-sectional shapes. The capillary flow in a closed system is described by two theoretical models that are provided [132]. Both the first and second models account for liquid imbibition into the paper matrix and flow through non-absorbing surfaces (flow in the gap). Significant conformity between the experimental results and the model solutions was found. The provided volume to the flow on the non-absorbing surface was shown to have an impact that improved the forecasts. The influence was found to be minimal at low flow rates but strong at high flow rates. This work demonstrates that the flow dynamics are influenced when a casing is added to a device, despite the fact that several experiments on flow in PADs were carried out on open systems. Employing various width sheets of filter paper, Patari et al. [124] conducted experimental and computational research on the wicking height and mass. Given that there is a linear relationship between wicking height and mass, it is convenient to evaluate the effective porosity. The proposed model with evaporation was required in order to explain the foundations of flowing fluid in testing paper and to provide relevant and useful benchmarks for the creation of PAD. Rosenfeld et al. [133] described an analytical and experimental investigation of a brand-new PAD for sample focusing by isotachopheresis. The author demonstrated that peak enhancement by significant sample focusing (on the order of 1000-fold) may be accomplished in a matter of minutes, despite the fact that dispersion was far more significant in paper than in glass. A handy figure of merit was provided by our analytical approach for assessing the effectiveness of ITP focusing. They demonstrated that, despite the stated improvements, the device’s efficiency was only about 10 percent, meaning the amount of sample accumulated was well below the theoretical upper limit. In microgravity, the phenomenon of absorption in a porous substrate underneath the presence of capillary forces was

studied [134]. The impact of non-stationary and convective factors on the imbibition process is examined in the analysis of the momentum conservation equation. The outcomes of numerical modeling of the recurrent imbibition process under the influence of capillary forces in microgravity in an irregularly shaped porous material are reported. The mathematical model of the imbibition phenomenon was presented by More et al. [135] to compare the saturation level for different time and distance levels that have been discussed between homogeneous and heterogeneous porous medium for various types of sands. Numerous natural and industrial processes can be benefited from spontaneous imbibition. Using the phase-field method, numerical simulations of counter-current absorption in porous media with various pore structures were carried out [136]. According to the simulation results, heterogeneous porous medium produced more oil than homogeneous porous media did. According to evidence, counter-current imbibition was significantly influenced by the differential between capillary driving pressure and capillary back pressure, which were both directly related to the pore structure and pore size distribution of porous media. Wang et al. [137] used numerical simulation to examine the paper-based microfluidic fuel cells in both transient and steady-state modes. Additionally, the effects of several structural characteristics on cell performance, such as electrode spacing, the distance between the electrode and the inlet, channel thickness, and electrode length, were also explored. The findings accelerated the development of microfluidic fuel cells by serving as both a theoretical foundation and a point of reference for the next optimization efforts.

5 Applications

5.1 Medical diagnosis

Point-of-care (POC) diagnosis is crucial for both the diagnosis and treatment of diseases. The objective of POC is to offer a solution when a sample is delivered to the equipment to make an informed decision. The main goal of paper-based microfluidics is to give developing nations a platform for low-cost illness diagnostics and environmental monitoring. It emerged as less priced, simple to use, and portable analytical test equipment. The development of medical science is aided by cutting-edge research in the field of PAD that provide quick, effective POC diagnostics. Due to the appealing features of PADs (low cost, no external pumping system needed, multiplexed assays, etc.) and their clinical applications, their range has expanded to POCs in resource-poor environments, home medical care, and severe disease biomedical diagnosis. However, the technology is semi-ready, and it still needs further development to achieve proper quantitative analysis. Here are some of the most important applications of PAD in the medical field:

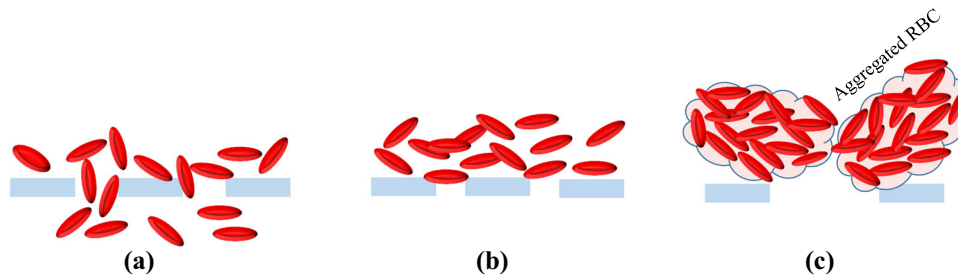


Fig. 13 Schematic diagram of the RBC agglutination to increase the effectiveness of filtration to separate blood plasma from entire blood. **a** Due to their deformability, RBCs can pass freely via filters. **b** RBCs cannot pass through filtration with pores smaller than 2.5 μm , while the flow of segregated plasma is severely hampered by small pores. **c** Large multicellular aggregates made of agglutinated RBCs might be removed utilising filters with large-diameter pores, allowing for faster flow rates of segregated plasma through the filters

5.1.1 Plasma separation

Since most medical diagnoses require a blood test as a prerequisite or necessary step, blood is the most important clinical analyte. The accurate interpretation of blood can deliver extensive information about a candidate's physiological state, enabling effective pathological diagnosis. The examination of blood, which is a complicated mixture of red blood cells, white blood cells, plasma, and other necessary components, is challenging. Because it transports all the vitamins, proteins, and minerals throughout the body, it controls all hemostatic and physiological parameters and could be used as a diagnostic analyte. First, the serum must be isolated from whole blood to be clinically diagnosed. For diagnosing either erythrocyte-related information or a routine concern of the other blood constituents excluding the erythrocytes, the separation of plasma from that of the whole blood is always the first step. Due to the presence of erythrocytes during the diagnosis, it is frequently difficult to detect a complex analyte like blood utilizing colorimetric, fluorescence, and chemiluminescence methods. These red blood cells may agglutinate and interfere with biochemical processes, as well as convert chemical signals to optical signals when used with color-based or optical-based sensing technologies. Erythrocytes influence the rheological dynamics of the blood in electrochemical detection situations. Therefore, separating the plasma from the erythrocytes is a step that must be taken while diagnosing blood. The use of RBC-specific adherent membranes, which permit plasma to pass through the paper, is the most used method for separating RBCs [138]. To separate RBCs from whole blood, electrochemical techniques [139] and agglutination reagent [140] have attracted interest as they could directly operate the whole blood sample as shown in Fig. 13. A cheap paper-based platform was created by Kar et al. [141] to extract blood plasma from a whole blood sample. They created a paper gadget based on the elegant separation method and the straightforward origami method, where the complete device is built by folding a single sheet of flat paper. This technique can be used to quickly identify sick states in blood samples without the use of experienced

workers or specialized lab settings. Another device for separating plasma from whole blood and determining glucose concentration was described [142]. This device does not require a membrane to separate the plasma from the whole blood sample and will be helpful in creating POC testing equipment that can identify analytes in small sample quantities. A BPS PAD was created by Burgos et al. [143] to identify and measure the S100B biomarker in peripheral whole blood. The VF2 collecting pad, which conducts vertical and lateral plasma separation was added with the complete blood sample. As a result of the cells creating and becoming trapped in the VF2 matrix due to hypertonic circumstances, the addition of NaCl to the VF2 pad causes RBCs to aggregate and increased plasma wicking.

5.1.2 Blood typing

The classification of blood due to the presence of antibodies and hereditary antigenic compounds on the surface of red blood cells is known as blood typing. For several medical operations, including blood transfusion and transplantation, it is important to know your blood type [144]. The situations of hemolytic transfusion reactions and other deadly outcomes can be avoided with the accurate identification of blood groups. The earliest techniques for blood typing relied on laboratory-based equipment, which does not adhere to WHO's ASSURED recommendations. Gel columns [145], thin-layer chromatography (TLC)-immunostaining [146], are the traditional blood-typing methods. In order to determine the blood type using agglutinated and nonagglutinated red blood cells. Khan et al. [147] proposed an inexpensive, appealing paper-based alternative. A piece of paper that had been treated with an antibody was the subject of an investigation by Jarujamrus et al. [148] The network of paper fibers becomes tangled with a mass of agglutinated cells that are produced when antibodies are desorbed from cellulose fibers. The assay performance influencing variables have been investigated, including antibody stability, papermaking additives, and paper structure. Larpan et al. [149] simultaneously suggested a simple and low-cost PAD for phenotyping RBC antigens. Using this Rh typing method, five

Rh antigens on RBCs can be recognised and observed under a microscope in less than 12 min. The suggested Rh phenotyping is dependent on the hemagglutination in the sample zones following immobilisation of the antibodies directed at each Rh antigen.

5.1.3 Detection of hormones in non-invasive body fluids

Non-invasive fluids are defined as substances that exist out of the human body. These include human breast milk, saliva, perspiration, and urine. These fluids have also been used for monitoring blood sugar, diagnosing celiac disease, evaluating alteration in body fluids, measuring pH and sodium levels in saliva and sweat, determining body fluid dynamics, and more ([150–152], etc.). A DNA aptamer-based sensor was developed [153] to identify dopamine in urine. Duplex aptamer dissociation served as the method's foundation, in which dopamine in the urine caused the sensor to alter conformation and become released from the capture probe. Schonhorn et al. [154] created a sandwich immunoassay for the pregnancy biomarker (human chorionic gonadotropin) hCG detection in urine. The experiment involved a three-dimensional patterned piece of paper with unaltered and hydrophobic wax-printed sections. The detection limit for this colorimetric approach was 6.7 mIU/ml, and the detection range was 0–250 mIU/ml. Within 10 min, the test's findings were ready. A unique molecularly imprinted polymer (MIP) grafted PAD for the sensing of 17-E2, which are essential for female menstrual and estrous cycles, was created by Xiao et al. [155] by using 12 mL of acetonitrile as the solvent, and using the molar ratios of 12:12:1 for the crosslinker, functional monomer, and template molecule. The detection limit for 17-estradiol in samples of human milk and urine using this method was determined to be 0.25 g/l.

5.1.4 Detection of hormones in invasive body fluids

These bodily fluids are the liquids that remain in the body. These consist of pleural fluids, blood plasma, blood serum, cerebrospinal fluid, and ascitic fluid [156]. Other applications of invasive body fluids include glucose monitoring [157], proteome analysis [158], the creation of wearable electrochemically active biosensors [159], the detection of antibodies [160], postmortem toxicology profiles, the diagnosis of Alzheimer's disease using specific peptides [161], and the identification of biomarkers for various diseases. A device was created by Rattanarat et al. [162] to detect dopamine in serum samples using electrochemical paper that had been treated with sodium dodecyl sulfate. With a dynamic detection range of 1–100 μ M and a detection limit of 0.37 M, this three-layer device was a simple, affordable technique. Shao et al. [163] created a low-cost kit for quick PCT detection because procalcitonin (PCT) is frequently utilized as a detector for bacterial infection. This approach was created for quick on-site detection with quick results by combining a double antibody

sandwich immunofluorescent test with the traditional LFA.

The WHO designated the onset of a novel coronavirus disease to be a public health emergency of global concern in January 2020. A general strategy to stop the spread of the COVID-19 outbreak is to isolate the infected individuals using efficient diagnostic techniques; the commonly used diagnosis technique currently in use is RT-PCR. Paper-based devices, as opposed to RT-PCR, are analytical tools that may perform rapid and accurate biomolecular detection without the need for laboratory-grade equipment or trained personnel. A low-cost and easily available serological technique to detect SARS-CoV-2 humanized antibodies was developed [164]. In this study, a common serological assay technique, ELISA, was combined with paper-based devices and the synthesized SARS-CoV-2 nucleocapsid antigen was deposited on the PAD. The recombinant antigen on the device might bind to the target antibodies in the human serum and create an immunological complex. It only took 30 min to complete the colorimetric reaction using the tetramethylbenzidine substrate and horseradish peroxidase (TMB/HRP), which is substantially faster than a typical ELISA experiment (usually 1 to 2 h). Yang et al. [165] suggested a possible RNA-based POC diagnostic tool for COVID-19 detection that integrates a paper-based POC diagnostic tool and LAMP assay technology. Nasal swabs can be used by home quarantine patients to collect their infected specimens. The colorimetric outcome of the LAMP reaction can then be seen on paper with the addition of certain reagents. The user could submit the output to cloud storage through the Internet by using a mobile phone camera to record the colorimetric shift.

Using the *Francisella novicida* Cas9 enzyme [166], created a CRISPR-based diagnostic paper test strip for the detection of the N501Y mutation. This assay has the potential to be tailored to additional interesting mutations in addition to being able to identify SARS-CoV-2 infection with this mutation. Yakoh et al. [105] presented a paper-based electrochemical biosensor, outlining a label-free technique for S protein antigen detection. An origami platform was created using chromatography paper as the substrate, and carbon-based electrodes were printed on it. SARS-CoV-2 IgM was then immobilized at the working electrode that had been modified with graphene oxide for antigen binding.

Additionally, paper microfluidics and ELISA tests were coupled to allow for the detection and quantification of multiplex antibodies from an individual health serum sample. Gong et al. [167] carried this out utilizing a porous material and wax fabrication method for printing. It executes all the necessary ELISA test phases as well as the instrument-free sampling and monitoring of serum samples. A paper-based biosensor with gold-hybridized zinc oxide nanowires (ZnO NWs) was presented [168], in which the working electrode was a critical component (WE). In less than 30 min, our biosensor could distinguish between IgG antibody concentrations against the SARS-CoV-2 spike

glycoprotein S1 unit utilizing impedimetric signal variations. For the quick and accurate sensing of SARS-CoV-2 spike antigen, Liu et al. [169] created a novel lateral flow strip-integrated nanozyme and enzymatic chemiluminescence immunoassay-based chemiluminescence testing. The paper test is based on a potent Co-Fe@hemin-peroxidase nanozyme that catalyses chemiluminescence equivalent to native peroxidase HRP and boosts immune reaction signal.

5.1.5 Detection of other biomarkers

Monitoring of protein- and DNA-based indicator is one of the most rapidly expanding areas of research for POC detection. For the unique detection of active pharmacological components in antituberculosis (TB) medications, color bars were used [170]. Similar to this, Koesdjojo et al. [171] proposed a method for anti-malarial medication. To increase the enzymatic filtration of the HIV DNA tenfold in a short period of time, a PAD for the detection of HIV DNA was developed. Monitoring of protein- and DNA-based biomarkers is one of the most rapidly expanding areas of research for POC detection. The enzymatic preservation, element blending, and repressor polymerase amplification of HIV DNA processes are all combined on the paper by PAD.

The Zika virus (ZIKV) was tested on a platform created [172] using RT-LAMP, and the entire procedure was carried out on a microfluidic chip made of wax-printed paper. The paper fibers in the device could pretreat large size molecules when a volume of blood serum or urine was introduced. Furthermore, proteins and other cell pieces were left behind due to the significant negative polarity of the cellulose fibers in paper, while the viral RNA with negative charges migrated to the end of the channel. On a straightforward hot plate, the target nucleic acids were amplified, and the results of the amplification can be determined by gauging the intensity of the pH indicator dye that was added. The most frequent infection that causes gastroenteritis in children, rotavirus A, has also been detected using LAMP-based paper devices [173]. It simply took 30 min to finish the thermal RNA amplification and nucleic acid extraction on a plain paper disc. Rotavirus A positive amplification result is instantly visible to the unaided eye as rose-red on the paper.

5.2 Environmental monitoring

Environmental deterioration has recently become the top worry for environmentalists. Ample resources, such as power and water, are needed for both home and industrial activities due to the continuously growing population and progress of the human race. The side products and leftovers of industrialization are released into the ambiance at the same time in the form of hazardous gases and effluents. Therefore, it is urgently necessary to control and regulate the toxins, particularly in the ambiance fluid. Nie et al. [67] presented the first instance of a paper-based sensor designed for the

sensing of heavy metal in 2010. To move the sample through the device, they used screen-printed electrodes made from paper, on which microchannels were created using patterning methods. Mensah et al. [174] developed solid-contact ion-selective electrodes (SC-ISEs) based on a porous site to quantify Cd^{+2} , Ag^+ , and K^+ . To accomplish the specificity for the ions, PAD was equipped with a membrane that contains ionic sites, and traditional ionophores for Cd^{+2} , Ag^+ , and K^+ . Yu et al. [175] created a device based on the lamination approach to detect lead. A spatula was used to apply conductive electrodes to the paper after it had been cut out using a CO_2 laser to seep the ink into the paper. The electrode layer of PAD was then positioned between two more paper layers that had been sandwiched together and layered with the biodegradable polyester polycaprolactone (PCL). The resulting laminated electrodes were then permanently put together to provide a durable and practical device. Wang et al. [176] created a paper-based multianalyte detection system in 2018 using nitrocellulose paper (0.45 μ m pore size). The three-electrode cell used in the paper-based electrodes was created using the magnetron sputtering technique, which spat a thin layer of gold onto the paper. PAD's capabilities were initially tested for the purpose of detecting Cu^{+2} , which was then used to refine the voltammetric parameters. Studying the interference from Pb^{+2} , Cd^{+2} , Zn^{+2} , Bi^{+3} , Cl^- , Na^+ , and K^+ revealed that the Cu^{+2} signal decreased by up to 10 percent, reaching a value of 15 percent in the presence of Pb^{+2} , while still demonstrating the device's good performance. A separate methodology was proposed by Shimizu et al. [177] for quantification of phosphate over paper. The Murphy and Riley approach was used by the authors, and they took advantage of the P-Mo complex's creation in a solution before introducing the analyte and the reagents to the paper electrode. It has been demonstrated that using this method enables simultaneous increases in the active regions and unhindered redox processes. For the monitoring of paraoxon-ethyl in soil and fertilized soil samples, Cioffi et al. [178] created an electrochemical biosensor based on office paper. The sample required 100 L of aqueous solution (2 percent ethanol) for the treatment, accompanied by a vortex and filtration with an MF-Millipore Membrane Filter. The bio detector was able to detect quantities of 10 and 25 ng/mL in soil with recovery values of 84 percent and 97 percent, respectively, based on a signal-to-noise ratio of 3 in standard solutions.

A unique paper-based immunoassay was created for the accurate measurement of ethinyl estradiol (EE2) in water samples [179]. The silica nanoparticles were utilized to enhance the coating of biomolecule immobilization, enabling an improvement in their assimilation into the device and resulting in signal amplification. In order to capture and preconcentrate EE2, river water specimen were integrated to the amended layer of hydrophilic microzones as shown in Fig. 14. Paper microzones were then placed over the decreased graphene sheet on a carbon electrode that had been screen-printed. To desorbate the bound EE2, sulfuric

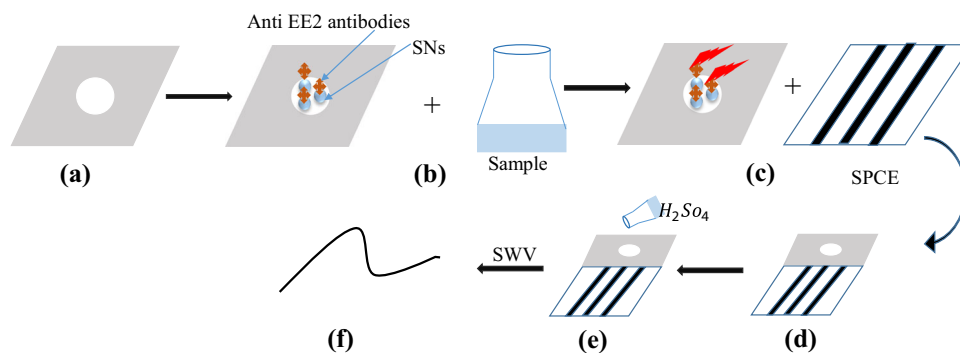


Fig. 14 Schematic diagram of the electrochemical paper-based immunocapture assay to determine the quantity of ethinylestradiol (EE2) in samples. **a** Paper microzones, **b** paper altered with anti-EE2 specific antibodies and silica nanoparticles (SNs) and then the addition of river water sample, **c** collect paper microzones to collect with the layer of reduced graphene on electrode **d** On the edge of reduced graphene, paper microzones were applied, **e** bound EE2 was dissolved by applying a weak acid solution to the paper, **f** electrochemical detection by square-wave voltammetry (SWV)

acid solution was placed to the paper microzones. The recovered EE2 was electrochemically detected using square-wave voltammetry, and the oxidation current that resulted was comparable to the EE2 level in the sample.

A paper-based instrument was created to detect the presence of diclofenac (DCF) in samples of spiked tap water [180]. A circular design was initially wax printed on paper before being heated to 100°C for one minute of curing. The reference and counter electrodes of the commercial connector were gold-plated pins spanning a piece of black plastic. The wires served as electrodes and a handy connection for the industrial interaction that was attached to the power supply unit. A clip was made by fusing the reference and counter electrodes together. By creating an 8 electrochemical cell framework for multiple observations, the idea's adaptability was shown.

5.3 Energy devices

Paper is a desirable material for energy storage devices due to its availability, minimal cost, readily disposed of, and environmentally acceptable due to the nonhazardous waste they produce. The most often used paper-based energy components include capacitors, cells, transistors, power stations, detectors, RFID tags, solar panel arrays, digital displays, and medical surveillance systems. Guo et al. [181] proposed a paper-based self-charging power unit that combines a paper-based triboelectric nanogenerator and a supercapacitor, to simultaneously harvest and store energy from body movement. However, these devices need to scale up for the generation of power in large quantities. Below are some of the most recent developments in creating energy devices based on the idea of paper-based microfluidics:

5.3.1 Batteries

POC devices must meet the ASSURED criteria of the WHO and be self-powered, integrated with power-generating units, and should be used without the use of any additional equipment. Thom et al. [78] demonstrated the first microfluidic device that could produce its own electricity when a sample was added. The device possesses fluidic channels with fluidic batteries built right in. These batteries were fabricated by stacking the various layers of the paper, with the electrodes, electrolyte, and salt bridge loaded into the appropriate paper sheet in a dry state.

Lee [79] created paper-based batteries by using copper as the current collector, magnesium foil for the anode, and filter paper coated with copper chloride for the cathode. A maximum voltage and power of 1.56 V and 15.6 mW were delivered by the battery when a sample of urine, saliva, or tap water was added. Paper-based batteries are appropriate for single-use ones since these batteries are activated upon the application of reagent, and the power output of batteries tends to decrease as reagent decays over time. Based on the idea of origami, Liu et al. [182] developed a self-powered ePAD that can detect glucose. The device integrates with a primary battery and can directly activate analyte solutions. A simple origami bacteria battery that can fold and unfold to accommodate various power requirements was proposed [183]. The device is filled with water or wastewater that has a very little amount of bacteria dissolved into it. As the liquid moves through the fluidic channels, it eventually reaches the batteries and produces electricity. Al-air battery is one of the great options among many various metal-air batteries available in the market. Shen et al. [184] integrated the idea of paper-based microfluidics with aluminum-air batteries in 2019 to eliminate the need for costly air electrodes or external pump devices. They sandwiched a piece of graphite foil coated with a catalyst between an anode made of aluminum foil and a cathode made of graphite foil. As shown in Fig. 15, an

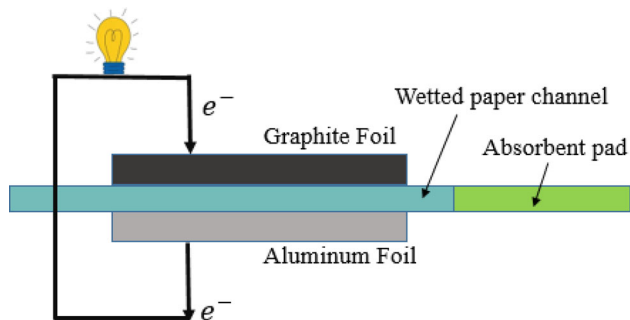


Fig. 15 Schematic representation of an aluminum foil anode, a catalyst-coated graphite foil cathode, and a thin sheet of fibrous capillary paper are sandwiched in a paper-based Al-air battery

absorbent pad was also employed with a paper channel to ensure a uniform flow of electrolytes.

Al-air battery on paper microfluidic channel demonstrates much-increased capacity when compared to traditional Al-air battery. A paper-based Al-air battery with a maximum power density of $21 \text{ mW}/\text{cm}^2$ was also reported by Wang et al. [185]. One flexible zinc-air battery containing a brand-new hollow channel construction was described by Yang et al [186]. To lower the internal resistance of ZABs, one hollow channel structure was successfully constructed and incorporated. The maximum power density of the hollow channel-based ZAB was $138 \text{ mW}/\text{cm}^2$, 283% greater than that of traditional P-ZABs. When the device was bent from 0° to 180° , it was capable of controlling a calculator. Wang et al. [80] created a 5-cell battery with an efficiency of up to 97% after discovering that Al corrosion could be stopped in an alkaline environment using paper-based delivery. This battery pack was successfully scaled up and used to illustrate how to charge portable electronics.

5.3.2 Fuel cells

It is a device that generates electricity through a chemical process. In contrast to batteries, cells do not deplete or require a recharge. The identification and application of sustainable and environmentally friendly energy supplies are required due to the rapid increase in energy consumption. Applications for wind energy, photovoltaics, and other renewable energy sources are constrained by their low efficiency. As a more efficient means of converting a fuel's chemical energy into electric power, fuel cells have emerged as a superior alternative for generating energy. These microfluidic fuel cells include chemical sensors in addition to being employed with communication and transportation systems. Zebda et al. [187] proposed an enzyme-based micro fuel cell in which electrodes were positioned along the catholyte and anolyte streams of the fuel and oxidant streams in the Y-direction. While glucose oxidase worked at the anode to oxidize glucose, laccase worked at the cathode to reduce O_2 . Noh and Shim [188]

reported another enzymatic fuel cell by immobilizing enzyme (glucose oxidases) molecules to the electrode surface in order to further lower the cost and extend the life of the fuel cell up to 16 days. The power density and open circuit voltage produced by the conversion of glucose into gluconic acid and hydrogen peroxide are $0.78 \text{ mW}/\text{cm}^2$ and 0.48 V, respectively. Using graphite electrodes attached to conductive wires through silver adhesive paste on a Y-shaped filter paper strip, Arun et al. [189] created a capillarity-mediated fuel cell. Inlet channels were soaked in a solution of sulfuric acid (oxidant) and formic acid (fuel). Formic acid produced $32 \text{ mW}/\text{cm}^2$ of electricity for more than 15 h by utilizing 1 mL of fuel. On the anode, formic acid broke down into CO_2 and electrons, which were then transmitted to the cathode by the external circuit. Based on the idea of reversed electro dialysis, Chang et al. created a multi-layered paper device for energy harvesting. This approach uses asymmetric ion transport through ion-selective membranes to extract energy from two solutions with varying salt contents. A voltage differential across the membrane is caused by the concentration difference, which generates electricity. Wax was used to define the flow, and the paper was coated with Ag/AgCl ink to create the electrodes. When a potassium chloride concentration gradient (0.1 mM/100 mM) was applied across the membrane of the device, which uses an ion-selective membrane placed between two layers of wax-printed paper, the device produced a power density of $275 \text{ nW}/\text{cm}^2$. In order to control the capillary flow on paper, Wang et al. [137] proposed coupling the microfluidic channel outputs with a photothermal module for water evaporation. As a proof of concept, prototype paper-based microfluidic fuel cells coupled to a photothermal module are created. Their peak power density can rise when exposed to simulated sunlight. The recent research opens a new avenue for controlling the functionality of PAD, a problem that has long existed in this field. It not only provides a realistic way to improve the efficiency of solar-powered paper-based microfluidic fuel cells.

5.4 Food quality

One of the essentials of life is food, and the nutritional content of the food is quite important for ensuring a healthy lifestyle. As a result, access to high-quality, safe foods is a must for human existence. Both physical and mental health can be maintained with food. Food safety has become one of the most critical challenges in the world due to the introduction of numerous chemical dangers to improve the flavor or aesthetic look of food, satisfy high market demand, and reduce costs. The issue of poor food quality is more serious in developing nations, especially in rural regions. Therefore, diagnosis technology must be affordable, portable, and small. The amounts of nitrite, a preservative used to give the meat a fresh appearance and extend shelf life were determined [190]. A wax stamping technique was used to create a paper-based microplate. The Griess

reagents, which generate a pink color when reacting with nitrite ions in food, were then put in each microzone as colorimetric markers. The amount of nitrite present in the meat directly correlated with the intensity of the resulting pink color. By analyzing the coffee-ring effect of the produced colors on the well plates, Trofimchuk et al. [191] improved the limit of detection for a similar device. As low as 1.1 mg/kg was determined to be the detection limit of this test for nitrite in pork, demonstrating the potential uses of regularly checking the nitrite level in meat samples. For the colorimetric detection of amylose content in rice, Hu et al. [192] created PADs. Their suggested technique of detection was based on the interaction between amylose and iodine, which might result in an amylose-iodine complex with an obvious blue color. They demonstrated that this method may be used to evaluate rice products with an accuracy of 6.3% and amylose levels ranging from 1.5 to 26.4%. Nogueira et al. [193] used a redox titration technique to colorimetrically identify the alcohol concentration of whiskey samples on PADs. In this reaction, the amount of oxalic acid consumed during the back-titration was used to indirectly quantify the amount of ethanol in whiskey while taking the stoichiometric ratio into account. They have demonstrated that their suggested detection approach, which has a detection limit of 2.1% at the point of need, is affordable and only needs a tiny amount of reagent to precisely assess the concentration of ethanol in an alcoholic beverage. For the simultaneous spot test analysis of boric acid, maltodextrin, and hydrogen peroxide, Patari, and Mahapatra [194] designed a paper test card. Using a laser printer to print toner ink, hydrophobic channels with a 14 mm diameter were created on Whatman Grade 4 filter sheets. A camera was used to take pictures of the reaction zone to assess the color variation of the area. The reaction zone will turn orange, bluish chocolate, and brown depending on the presence of boric acid, maltodextrin, and H_2O_2 . A μ PAD the concurrent calorimetric measurement of urea, H_2O_2 , and pH was published by Guinati et al. [195]. To ensure that the paper was completely cut without any surface damage, the EVA-coated polyester Gazela laminator model was used to laminate the paper at 140°C. Then a layout of the 'PAD' was created to be cut out using a craft cutter printer, which can produce gadgets quickly, cheaply, and with a minimum amount of technical equipment. The software version was used to analyze the digital photographs after they had all been digitized at a resolution of 600 dpi. Despite the numerous benefits provided by paper-based devices, there is still much room for technology development. Colorimetric detection methods are commonly used in PADs, which makes getting quantitative results difficult. Furthermore, when it comes to PAD-based energy generation, the technology is semi-ready and needs to be scaled up.

6 List of PADs successfully demonstrated for diverse applications

The devices are small, light, portable, and cost little to manufacture, use, and dispose of. Low reagent and analyte consumption is a unique benefit of microfluidics. A wide range of practical applications has been found for them in a variety of research fields: chemistry, biochemistry, genomics, forensics, toxicology, immunology, environmental studies, and biomedicine. Microfluidics have been used successfully in the past in the clinical analysis of blood, the detection and identification of infections, proteins, and environmental toxins, genetic research, and in the pharmaceutical sector. The analytical and diagnostic capabilities of these simple devices may revolutionize medicine and pharmaceuticals. Therefore, providing a list of PADs (specifically for clinical and home applications) which has been successfully demonstrated at least at the laboratory level.

7 Limitations

The outstanding qualities of paper-based microfluidic devices made them suitable for an endless number of applications. However, due to the characteristics of paper, fabrication processes, analytes chosen, and sensing techniques used in the devices, μ PADs do have some limitations. In addition, major drawbacks of paper-based devices include sample retention in fluidic channels and significant sample evaporation during operation, both of which reduce device efficiency. The amount of sample needed increases because only about half of the entire introduced sample volume reaches the detecting zone. The effectiveness of some patterning techniques is greatly influenced by the environment in which the device will be used, and the effectiveness of some hydrophobic chemicals is insufficient to create robust hydrophobic barriers that can tolerate samples with different properties. When a liquid with low surface tension comes into contact with wax channels, the liquid starts to penetrate even in hydrophobic parts, whereas the hydrophobic channels or AKD only function properly for particular liquids with surface tension higher than a critical value. This phenomenon occurs as wax creates hydrophobicity by obstructing the pores of paper and lowering the surface energy of paper to effectively direct liquids. Without highly skilled and experienced people, comparison-based detection methods cannot produce accurate results. Various detection techniques are unable to pick up contamination in samples with low contamination levels. These are the present drawbacks of paper-based microfluidic technology that must be overcome.

Table 2 List of ‘ μ PADs’

Field-up application	Short description
Medical diagnosis	Antibody screening tool that shows whether a patient has a contagious disease infection and an immune reaction to it [196]
Medical diagnosis	Devices used to identify uropathogenic <i>E. coli</i> rely on the ability to detect nitrite, which is produced when <i>E. coli</i> reduces nitrate. [197]
Food quality control	Pesticide detection sensor made of paper for crop samples [198]
Food quality control	3D PAD for identifying the milk allergen casein [199]
Food quality control	Colorimetric PAD to detect <i>Salmonella</i> [200]
Medical diagnosis	A pop-up, DNA-based, label-free ePAD for HBV (a biomarker of liver disorders) detection [201]
Medical diagnosis	A vertical flow-based paper sandwich-type immunosensor for sensing of influenza H1N1 viruses [202]
Food quality control	Instrument to measure aluminium in water without pre-treatment or pre-concentration of the sample [203]
Medical diagnosis	PAD for detection of malaria [204]
Medical diagnosis	Device for medical diagnosis and sweat analysis that simultaneously measures glucose, lactate, pH, chloride, and volume [205]
Medical diagnosis	Platform for electrochemical immunosensing for pmol/L Ebola virus detection [206]
Medical diagnosis	Human chorionic gonadotropin (a pregnancy indicator) detection via a PAD [207]
Medical diagnosis	PAD to immobilize different antibodies or anti-immunoglobulin E onto screen-printed carbon electrodes [208]
Medical diagnosis	PAD for COVID-19 diagnosis [209–211]
Medical diagnosis	Biosensor for POC sensing of dengue virus [212]
Food quality control	PAD to track total ammonia in fish pond water [213]
Medical Diagnosis	Electrochemical and self-powered paper-based device for glucose sensing [214, 215]
Medical diagnosis	PAD for eliminating the necessity for a micropipette in quantitative analysis [216]
Medical diagnosis	PAD to extract blood plasma from a whole blood sample [138]
Medical diagnosis	A disposable ePAD for quantification of albumin in a urine sample [217]
Food quality control	3D PAD to simultaneously detect multiple chemical adulterants in milk [195, 218]
Medical diagnosis	An intelligent paper-based UV monitor that can detect the solar UV intensity in real time for human health and safety [219]
Food quality control	For estimation of the peroxide value in vegetable oils using colorimetric PAD [220]
Medical diagnosis	Using exhaled air, an ePAD wearable sensor can detect hydrogen peroxide in real time [221]
Food quality control	<i>Escherichia coli</i> and <i>Staphylococcus aureus</i> , the two main pathogenic bacteria that cause milk poisoning, can be found using a colorimetric PAD [222]
Medical diagnosis	PAD for blood typing. [129, 147, 185]
Medical diagnosis	Detection of 17-E2, which is crucial for female menstrual and estrous cycles [155]
Medical diagnosis	Peptide-based Alzheimer’s diagnostic device [161]
Energy generation	A power unit that incorporates a paper-based supercapacitor and a triboelectric nanogenerator (TENG) to concurrently harvest and store energy from the movement [181]
Food quality control	Device to detect the presence of diclofenac (DCF) in samples of spiked tap water [179]
Energy generation	Paper-based batteries with maximum voltage and power of 1.56 V and 15.6 mW [78]
Food quality control	Device to detect the amount of nitrite, a preservative used in meat [190, 191]
Food quality control	Device based on redox titration technique to calorimetrically identify the alcohol concentration of whiskey samples [193]

8 Conclusion

Paper is meeting the optimum foundation material requirement for bringing this technology from the lab to the market due to the development of new fabrication protocols for PADs. Litmus paper is among the first papers to be used in chemical analysis. Despite being widely used, litmus paper was a revolutionary invention at the time because it made possible accurate pH measurements. Analytical devices began to be developed slowly with one of the most notable developments being the LFA, which was first industrialized as an over-the-counter pregnancy test in 1975 [223]. In 2007, Whitesides' group published a paper that ignited the field [1]. The paper-based devices meet WHO specifications for diagnostic devices used in developing countries. According to WHO, the device should be ASSURED, that is, affordable, sensitive, specific, user-friendly, rapid and robust, equipment-free, and deliverable. Paper enables fluid flow without pumps, purification, electrode stabilization, and other applications. Paper devices can be equipment-free if consider integrated devices or colorimetric detection, with the exception of capillary forces that render external pumping obsolete. The devices are portable because the paper is thin, and it is also widely available worldwide. Consider that fully integrated, reusable, sensing platforms will soon be available as paper-based electronics advance. This review discusses the fabrication methods and detection modes in detail. We also discussed recent advances in μ PAD for POC diagnostics, food quality control, power generation, and environmental control with theoretical analysis of fluid flow in paper. With minor changes to the device design and fabrication methods, PADs can be effectively implemented for the analysis of basic and extensive systems. There are several issues that remain despite advancements in paper-based microfluidic technology. Fabrication of μ PADs requires the printing of hydrophilic paper by using methods like photolithography, screen printing, etc to control the flow of liquid in the appropriate manner. Although these patterning methods can efficiently define the flow in a porous substrate, various other fabrication techniques are also required for the successful mass production of these devices. Therefore, large-scale printing methods should be investigated to fabricate μ PADs with multi-layer complex structures that can be made at low cost, high resolution, and with easy process steps. It will be difficult to achieve the big goals discussed above. The field must continue to develop in the future, focusing on both basic and applied research areas while also considering the elements needed for industrialization. Materials science has a chance to contribute more to fundamental research by improving techniques for controlling the reactivity of devices using materials building and surface alteration. Although several papers manufactured from different natural or synthetic fibres have been created, PADs are still widely applied in biosensor applications. Fiber-based materials have mechanical stability, a hydrophobic interface, porosity, and the

capacity to change the texture through interaction with biorecognition molecules. Some examples of these materials include Teflon, glass fibres, graphene and graphene oxide, polypropylene, poly(lactic acid), and carbon nanotubes. The ongoing exploration of hybrid devices that combine various materials and flow patterns and a detailed understanding of circulation in these systems will enable the creation of new systems from first principles instead of using a considerably slower empirical approach. It is critical from a translational perspective to keep broadening the PAD usage field with an emphasis on applications where PADs actually bring value that is unique from other technologies. By approaching it from this angle, you'll be able to enter the marketplace more quickly and potentially effect real change.

References

1. A.W. Martinez, S.T. Phillips, M.J. Butte, G.M. Whitesides, Patterned paper as a platform for inexpensive, low-volume, portable bioassays. *Angew. Chem.* **119**(8), 1340–1342 (2007)
2. A.W. Martinez, S.T. Phillips, G.M. Whitesides, E. Carrilho, Diagnostics for the developing world: microfluidic paper-based analytical devices (2010)
3. A. Tay, A. Pavesi, S.R. Yazdi, C.T. Lim, M.E. Warkiani, Advances in microfluidics in combating infectious diseases. *Biotechnol. Adv.* **34**(4), 404–421 (2016)
4. D. Mark, S. Haeberle, G. Roth, F.v. Stetten, R. Zengerle, Microfluidic lab-on-a-chip platforms: requirements, characteristics and applications. *Microfluid. Based Microsyst.* pp. 305–376 (2010)
5. B. Bhushan, in *Springer handbook of nanotechnology* (Springer, 2017), pp. 1–19
6. D. Lin, B. Li, J. Qi, X. Ji, S. Yang, W. Wang, L. Chen, Low cost fabrication of microfluidic paper-based analytical devices with water-based polyurethane acrylate and their application for bacterial detection. *Sens. Actuators B: Chem.* **303**, 127,213 (2020)
7. A.W. Martinez, S.T. Phillips, G.M. Whitesides, Three-dimensional microfluidic devices fabricated in layered paper and tape. *Proc. Natl. Acad. Sci.* **105**(50), 19606–19611 (2008)
8. A.W. Martinez, S.T. Phillips, B.J. Wiley, M. Gupta, G.M. Whitesides, Flash: a rapid method for prototyping paper-based microfluidic devices. *Lab Chip* **8**(12), 2146–2150 (2008)
9. E. Carrilho, S.T. Phillips, S.J. Vella, A.W. Martinez, G.M. Whitesides, Paper microzone plates. *Anal. Chem.* **81**(15), 5990–5998 (2009)
10. Y. Lu, W. Shi, L. Jiang, J. Qin, B. Lin, Rapid prototyping of paper-based microfluidics with wax for low-cost, portable bioassay. *Electrophoresis* **30**(9), 1497–1500 (2009)
11. Y. He, Y. Wu, J.Z. Fu, W.B. Wu, Fabrication of paper-based microfluidic analysis devices: A review. *RSC Adv.* **5**(95), 78109–78127 (2015)

12. Y. Yang, E. Noviana, M.P. Nguyen, B.J. Geiss, D.S. Dandy, C.S. Henry, based microfluidic devices: emerging themes and applications. *Anal. Chem.* **89**(1), 71–91 (2017)
13. T. Songjaroen, W. Dungchai, O. Chailapakul, W. Laiwattanapaisal, Novel, simple and low-cost alternative method for fabrication of paper-based microfluidics by wax dipping. *Talanta* **85**(5), 2587–2593 (2011)
14. E. Carrilho, A.W. Martinez, G.M. Whitesides, Understanding wax printing: a simple micropatterning process for paper-based microfluidics. *Anal. Chem.* **81**(16), 7091–7095 (2009)
15. V. Mani, K. Kadimisetty, S. Malla, A.A. Joshi, J.F. Rusling, based electrochemiluminescent screening for genotoxic activity in the environment. *Environ. Sci. Technol.* **47**(4), 1937–1944 (2013)
16. P. Kaewarsa, W. Laiwattanapaisal, A. Palasuwan, D. Palasuwan, A new paper-based analytical device for detection of glucose-6-phosphate dehydrogenase deficiency. *Talanta* **164**, 534–539 (2017)
17. K. Yamada, T.G. Henares, K. Suzuki, D. Citterio, Paper-based inkjet-printed microfluidic analytical devices. *Angew. Chem. Int. Ed.* **54**(18), 5294–5310 (2015)
18. K. Abe, K. Suzuki, D. Citterio, Inkjet-printed microfluidic multianalyte chemical sensing paper. *Anal. Chem.* **80**(18), 6928–6934 (2008)
19. L. Bai, Z. Xie, W. Wang, C. Yuan, Y. Zhao, Z. Mu, Q. Zhong, Z. Gu, Bio-inspired vapor-responsive colloidal photonic crystal patterns by inkjet printing. *ACS Nano* **8**(11), 11094–11100 (2014)
20. K. Maejima, S. Tomikawa, K. Suzuki, D. Citterio, Inkjet printing: an integrated and green chemical approach to microfluidic paper-based analytical devices. *RSC Adv.* **3**(24), 9258–9263 (2013)
21. A. Maattanen, P. Ihalainen, P. Pulkkinen, S. Wang, H. Tenhu, J. Peltonen, Inkjet-printed gold electrodes on paper: characterization and functionalization. *ACS Appl. Mater. Interfaces.* **4**(2), 955–964 (2012)
22. V. Mani, B. Paleja, K. Larbi, P. Kumar, J.A. Tay, J.Y. Siew, F. Inci, S. Wang, C. Chee, Y.T. Wang et al., Microchip-based ultrafast serodiagnostic assay for tuberculosis. *Sci. Rep.* **6**(1), 1–11 (2016)
23. C. Renault, X. Li, S.E. Fosdick, R.M. Crooks, Hollow-channel paper analytical devices. *Anal. Chem.* **85**(16), 7976–7979 (2013)
24. G. Chitnis, Z. Ding, C.L. Chang, C.A. Savran, B. Ziaie, Laser-treated hydrophobic paper: an inexpensive microfluidic platform. *Lab Chip* **11**(6), 1161–1165 (2011)
25. S. Das, R. Bhatia et al., based microfluidic devices: fabrication, detection, and significant applications in various fields. *Rev. Anal. Chem.* **41**(1), 112–136 (2022)
26. D.A. Bruzewicz, M. Reches, G.M. Whitesides, Low-cost printing of poly (dimethylsiloxane) barriers to define microchannels in paper. *Anal. Chem.* **80**(9), 3387–3392 (2008)
27. V. Faustino, S.O. Catarino, R. Lima, G. Minas, Biomedical microfluidic devices by using low-cost fabrication techniques: a review. *J. Biomech.* **49**(11), 2280–2292 (2016)
28. R. Amin, F. Ghaderinezhad, C. Bridge, M. Temirel, S. Jones, P. Toloueinia, S. Tasoglu, Pushing the limits of spatial assay resolution for paper-based microfluidics using low-cost and high-throughput pen plotter approach. *Micromachines* **11**(6), 611 (2020)
29. J. Olkkonen, K. Lehtinen, T. Erho, Flexographically printed fluidic structures in paper. *Anal. Chem.* **82**(24), 10246–10250 (2010)
30. P. de Tarso Garcia, T.M.G. Cardoso, C.D. Garcia, E. Carrilho, W.K.T. Coltro, A handheld stamping process to fabricate microfluidic paper-based analytical devices with chemically modified surface for clinical assays. *Rsc Adv.* **4**(71), 37,637–37,644 (2014)
31. T. Akyazi, J. Saez, J. Elizalde, F. Benito-Lopez, Fluidic flow delay by ionogel passive pumps in microfluidic paper-based analytical devices. *Sens. Actuators, B Chem.* **233**, 402–408 (2016)
32. V.F. Curto, N. Lopez-Ruiz, L.F. Capitan-Vallvey, A.J. Palma, F. Benito-Lopez, D. Diamond, Fast prototyping of paper-based microfluidic devices by contact stamping using indelible ink. *RSC Adv.* **3**(41), 18811–18816 (2013)
33. Y. Sameenoi, P.N. Nongkai, S. Nouanthavong, C.S. Henry, D. Nacapricha, One-step polymer screen-printing for microfluidic paper-based analytical device (μ pad) fabrication. *Analyst* **139**(24), 6580–6588 (2014)
34. X. Li, J. Tian, T. Nguyen, W. Shen, based microfluidic devices by plasma treatment. *Anal. Chem.* **80**(23), 9131–9134 (2008)
35. Y. Chunfang, Y. Siyang, J. Yan, H. Qiaohong, C. Hengwu, Fabrication of paper-based microfluidic devices by plasma treatment and its application in glucose determination. *Acta Chim. Sinica* **72**(10), 1099–1104 (2014)
36. Y. Jiang, Z. Hao, Q. He, H. Chen, A simple method for fabrication of microfluidic paper-based analytical devices and on-device fluid control with a portable corona generator. *RSC Adv.* **6**(4), 2888–2894 (2016)
37. P.K. Kao, C.C. Hsu, One-step rapid fabrication of paper-based microfluidic devices using fluorocarbon plasma polymerization. *Microfluid. Nanofluid.* **16**(5), 811–818 (2014)
38. P. Kwong, M. Gupta, Vapor phase deposition of functional polymers onto paper-based microfluidic devices for advanced unit operations. *Anal. Chem.* **84**(22), 10129–10135 (2012)
39. G. Demirel, E. Babur, Vapor-phase deposition of polymers as a simple and versatile technique to generate paper-based microfluidic platforms for bioassay applications. *Analyst* **139**(10), 2326–2331 (2014)
40. B. Chen, P. Kwong, M. Gupta, Patterned fluoropolymer barriers for containment of organic solvents within paper-based microfluidic devices. *ACS applied materials & interfaces* **5**(23), 12701–12707 (2013)
41. Y. Jiang, *Study on fabrication of microfluidic paper-based analytical devices and manipulation of microfluidic flow in paper-based channels using a hand-held corona treater* (ZheJiang University, HangZhou, China, 2014)
42. A.W. Martinez, S.T. Phillips, Z. Nie, C.M. Cheng, E. Carrilho, B.J. Wiley, G.M. Whitesides, Programmable diagnostic devices made from paper and tape. *Lab Chip* **10**(19), 2499–2504 (2010)

43. P. Kauffman, E. Fu, B. Lutz, P. Yager, Visualization and measurement of flow in two-dimensional paper networks. *Lab Chip* **10**(19), 2614–2617 (2010)
44. E. Fu, B. Lutz, P. Kauffman, P. Yager, Controlled reagent transport in disposable 2d paper networks. *Lab Chip* **10**(7), 918–920 (2010)
45. J. Tian, D. Kannangara, X. Li, W. Shen, Capillary driven low-cost v-groove microfluidic device with high sample transport efficiency. *Lab Chip* **10**(17), 2258–2264 (2010)
46. B.J. Toley, B. McKenzie, T. Liang, J.R. Buser, P. Yager, E. Fu, Tunable-delay shunts for paper microfluidic devices. *Anal. Chem.* **85**(23), 11545–11552 (2013)
47. J. Houghtaling, T. Liang, G. Thiessen, E. Fu, Dissolvable bridges for manipulating fluid volumes in paper networks. *Anal. Chem.* **85**(23), 11201–11204 (2013)
48. S. Jahanshahi-Anbuhi, A. Henry, V. Leung, C. Sicard, K. Pennings, R. Pelton, J.D. Brennan, C.D. Filipe, based microfluidics with an erodible polymeric bridge giving controlled release and timed flow shutoff. *Lab Chip* **14**(1), 229–236 (2014)
49. E. Fu, S.A. Ramsey, P. Kauffman, B. Lutz, P. Yager, Transport in two-dimensional paper networks. *Microfluid. Nanofluid.* **10**(1), 29–35 (2011)
50. B.R. Lutz, P. Trinh, C. Ball, E. Fu, P. Yager, Two-dimensional paper networks: programmable fluidic disconnects for multi-step processes in shaped paper. *Lab Chip* **11**(24), 4274–4278 (2011)
51. A. Apilux, Y. Ukita, M. Chikae, O. Chailapakul, Y. Takamura, Development of automated paper-based devices for sequential multistep sandwich enzyme-linked immunosorbent assays using inkjet printing. *Lab Chip* **13**(1), 126–135 (2013)
52. X. Li, P. Zwanenburg, X. Liu, Magnetic timing valves for fluid control in paper-based microfluidics. *Lab Chip* **13**(13), 2609–2614 (2013)
53. G.E. Fridley, H. Le, P. Yager, Highly sensitive immunoassay based on controlled rehydration of patterned reagents in a 2-dimensional paper network. *Anal. Chem.* **86**(13), 6447–6453 (2014)
54. C.E. Anderson, T. Huynh, D.J. Gasperino, L.F. Alonzo, J.L. Cantera, S.P. Harston, H.V. Hsieh, R. Marzan, S.K. McGuire, J.R. Williford et al., Automated liquid handling robot for rapid lateral flow assay development. *Anal. Bioanal. Chem.* **414**(8), 2607–2618 (2022)
55. A.C. Glavan, R.V. Martinez, E.J. Maxwell, A.B. Subramaniam, R.M. Nunes, S. Soh, G.M. Whitesides, Rapid fabrication of pressure-driven open-channel microfluidic devices in omniphobic rf paper. *Lab Chip* **13**(15), 2922–2930 (2013)
56. W. Liu, C.L. Cassano, X. Xu, Z.H. Fan, Laminated paper-based analytical devices (lpad) with origami-enabled chemiluminescence immunoassay for cotinine detection in mouse serum. *Anal. Chem.* **85**(21), 10270–10276 (2013)
57. E.I. Newsham, E.A. Phillips, H. Ma, M.M. Chang, S.T. Wereley, J.C. Linnes, Characterization of wax valving and μ piv analysis of microscale flow in paper-fluidic devices for improved modeling and design. *Lab on a Chip* (2022)
58. Q. Li, Y. Xu, J. Qi, X. Zheng, S. Liu, D. Lin, L. Zhang, P. Liu, B. Li, L. Chen, A self-powered rotating paper-based analytical device for sensing of thrombin. *Sensors and Actuators B: Chemical* **351**, 130,917 (2022)
59. W. Dungchai, O. Chailapakul, C.S. Henry, Electrochemical detection for paper-based microfluidics. *Anal. Chem.* **81**(14), 5821–5826 (2009)
60. A. Apilux, W. Dungchai, W. Siangproh, N. Praphairaksit, C.S. Henry, O. Chailapakul, Lab-on-paper with dual electrochemical/colorimetric detection for simultaneous determination of gold and iron. *Anal. Chem.* **82**(5), 1727–1732 (2010)
61. K.K. Jagadeesan, S. Kumar, G. Sumana, Application of conducting paper for selective detection of troponin. *Electrochem. Commun.* **20**, 71–74 (2012)
62. Y. Wu, P. Xue, Y. Kang, K.M. Hui, based microfluidic electrochemical immunodevice integrated with nanobioprobes onto graphene film for ultrasensitive multiplexed detection of cancer biomarkers. *Anal. Chem.* **85**(18), 8661–8668 (2013)
63. N.C. Sekar, S.A.M. Shaegh, S.H. Ng, L. Ge, S.N. Tan, A paper-based amperometric glucose biosensor developed with prussian blue-modified screen-printed electrodes. *Sens. Actuators, B Chem.* **204**, 414–420 (2014)
64. C. Renault, M.J. Anderson, R.M. Crooks, Electrochemistry in hollow-channel paper analytical devices. *J. Am. Chem. Soc.* **136**(12), 4616–4623 (2014)
65. N. Dossi, R. Toniolo, A. Pizzariello, E. Carrilho, E. Piccin, S. Battiston, G. Bontempelli, An electrochemical gas sensor based on paper supported room temperature ionic liquids. *Lab Chip* **12**(1), 153–158 (2012)
66. J.C. Cunningham, N.J. Brenes, R.M. Crooks, Paper electrochemical device for detection of dna and thrombin by target-induced conformational switching. *Anal. Chem.* **86**(12), 6166–6170 (2014)
67. Z. Nie, C.A. Nijhuis, J. Gong, X. Chen, A. Kumachev, A.W. Martinez, M. Narovlyansky, G.M. Whitesides, Electrochemical sensing in paper-based microfluidic devices. *Lab Chip* **10**(4), 477–483 (2010)
68. M. Santhiago, J.B. Wydallis, L.T. Kubota, C.S. Henry, Construction and electrochemical characterization of microelectrodes for improved sensitivity in paper-based analytical devices. *Anal. Chem.* **85**(10), 5233–5239 (2013)
69. N. Godino, R. Gorkin, K. Bourke, J. Ducree, Fabricating electrodes for amperometric detection in hybrid paper/polymer lab-on-a-chip devices. *Lab Chip* **12**(18), 3281–3284 (2012)
70. M. Santhiago, L.T. Kubota, A new approach for paper-based analytical devices with electrochemical detection based on graphite pencil electrodes. *Sens. Actuators, B Chem.* **177**, 224–230 (2013)
71. N. Dossi, R. Toniolo, F. Impellizzieri, G. Bontempelli, Doped pencil leads for drawing modified electrodes on paper-based electrochemical devices. *J. Electroanal. Chem.* **722**, 90–94 (2014)
72. G.P. Ciniciato, C. Lau, A. Cochrane, S.S. Sibbett, E.R. Gonzalez, P. Atanassov, Development of paper based electrodes: From air-breathing to paintable enzymatic cathodes. *Electrochim. Acta* **82**, 208–213 (2012)

73. L.Y. Shiroma, M. Santhiago, A.L. Gobbi, L.T. Kubota, Separation and electrochemical detection of paracetamol and 4-aminophenol in a paper-based microfluidic device. *Anal. Chim. Acta* **725**, 44–50 (2012)
74. S.E. Fosdick, M.J. Anderson, C. Renault, P.R. DeGregory, J.A. Loussaert, R.M. Crooks, Wire, mesh, and fiber electrodes for paper-based electroanalytical devices. *Anal. Chem.* **86**(7), 3659–3666 (2014)
75. J. Yang, Y.G. Nam, S.K. Lee, C.S. Kim, Y.M. Koo, W.J. Chang, S. Gunasekaran, fluidic electrochemical biosensing platform with enzyme paper and enzymeless electrodes. *Sens. Actuators, B Chem.* **203**, 44–53 (2014)
76. J. Lu, S. Ge, L. Ge, M. Yan, J. Yu, Electrochemical dna sensor based on three-dimensional folding paper device for specific and sensitive point-of-care testing. *Electrochim. Acta* **80**, 334–341 (2012)
77. S. Ge, L. Ge, M. Yan, X. Song, J. Yu, J. Huang, A disposable paper-based electrochemical sensor with an addressable electrode array for cancer screening. *Chem. Commun.* **48**(75), 9397–9399 (2012)
78. N.K. Thom, K. Yeung, M.B. Pillion, S.T. Phillips, “fluidic batteries” as low-cost sources of power in paper-based microfluidic devices. *Lab Chip* **12**(10), 1768–1770 (2012)
79. K.B. Lee, Urine-activated paper batteries for biosystems. *J. Micromech. Microeng.* **15**(9), S210 (2005)
80. Y. Wang, W. Pan, H.Y. Kwok, H. Zhang, X. Lu, D.Y. Leung, Liquid-free air-batteries with paper-based gel electrolyte: a green energy technology for portable electronics. *Journal of Power Sources* **437**, 226,896 (2019)
81. C. Zhao, M.M. Thuo, X. Liu, A microfluidic paper-based electrochemical biosensor array for multiplexed detection of metabolic biomarkers. *Science and technology of advanced materials* **14**(5), 054,402 (2013)
82. I. Ramfos, N. Vassiliadis, S. Bionas, K. Efstathiou, A. Fragoso, C.K. O’Sullivan, A. Birbas, A compact hybrid-multiplexed potentiostat for real-time electrochemical biosensing applications. *Biosens. Bioelectron.* **47**, 482–489 (2013)
83. C. Liu, F.A. Gomez, A microfluidic paper-based device to assess acetylcholinesterase activity. *Electrophoresis* **38**(7), 1002–1006 (2017)
84. T.M. Cardoso, R.B. Channon, J.A. Adkins, M. Talhavini, W.K. Coltro, C.S. Henry, A paper-based colorimetric spot test for the identification of adulterated whiskeys. *Chem. Commun.* **53**(56), 7957–7960 (2017)
85. E.F.M. Gabriel, P.T. Garcia, F.M. Lopes, W.K.T. Coltro, Based colorimetric biosensor for tear glucose measurements. *Micromachines* **8**(4), 104 (2017)
86. T.M. Cardoso, F.R. de Souza, P.T. Garcia, D. Rabelo, C.S. Henry, W.K. Coltro, Versatile fabrication of paper-based microfluidic devices with high chemical resistance using scholar glue and magnetic masks. *Anal. Chim. Acta* **974**, 63–68 (2017)
87. R. Meelapsom, P. Jarujamrus, M. Amatongchai, S. Chairam, C. Kulsing, W. Shen, Chromatic analysis by monitoring unmodified silver nanoparticles reduction on double layer microfluidic paper-based analytical devices for selective and sensitive determination of mercury (ii). *Talanta* **155**, 193–201 (2016)
88. K. Yamada, K. Suzuki, D. Citterio, Text-displaying colorimetric paper-based analytical device. *Acs Sensors* **2**(8), 1247–1254 (2017)
89. L.H. Mujawar, J. Dhavamani, M.S. El-Shahawi, A versatile optical assay plate fabricated from e-waste and its application towards rapid determination of Fe³⁺ ions in water. *New J. Chem.* **41**(18), 9731–9740 (2017)
90. M.A. Chowdury, N. Walji, M.A. Mahmud, B.D. MacDonald, based microfluidic device with a gold nanosensor to detect arsenic contamination of groundwater in Bangladesh. *Micromachines* **8**(3), 71 (2017)
91. C.C. Liu, Y.N. Wang, L.M. Fu, D.Y. Yang, Rapid integrated microfluidic paper-based system for sulfur dioxide detection. *Chem. Eng. J.* **316**, 790–796 (2017)
92. M.C. Carneiro, L.R. Rodrigues, F.T. Moreira, M.G.F. Sales, Colorimetric paper-based sensors against cancer biomarkers. *Sensors* **22**(9), 3221 (2022)
93. T. Mahmoudi, A.P. Tazehkand, M. Pourhassan-Moghaddam, M. Alizadeh-Ghods, L. Ding, B. Baradaran, S.R. Bazaz, D. Jin, M.E. Warkiani, Paper-free paper-based nanobiosensing platform for visual detection of telomerase activity via gold enhancement. *Microchemical Journal* **154**, 104,594 (2020)
94. A.C. Fu, Y. Hu, Z.H. Zhao, R. Su, Y. Song, D. Zhu, Functionalized paper microzone plate for colorimetry and up-conversion fluorescence dual-mode detection of telomerase based on elongation and capturing amplification. *Sens. Actuators, B Chem.* **259**, 642–649 (2018)
95. W. Fernando, H. Jayarathna, M. Kaumal, Low-cost microfluidic electrochemical paper-based device to detect glucose. *Journal of Science of the University of Kelaniya Sri Lanka* **15**(1) (2022)
96. W.T. Fonseca, K.R. Castro, T.R. de Oliveira, R.C. Faria, Disposable and flexible electrochemical paper-based analytical devices using low-cost conductive ink. *Electroanalysis* **33**(6), 1520–1527 (2021)
97. M.R. Tomei, S. Cinti, N. Interino, V. Manovella, D. Moscone, F. Arduini, based electroanalytical strip for user-friendly blood glutathione detection. *Sens. Actuators, B Chem.* **294**, 291–297 (2019)
98. N. Ruecha, K. Shin, O. Chailapakul, N. Rodthongkum, Label-free paper-based electrochemical impedance immunosensor for human interferon gamma detection. *Sens. Actuators, B Chem.* **279**, 298–304 (2019)
99. H. Wang, C. Zhou, X. Sun, Y. Jian, Q. Kong, K. Cui, S. Ge, J. Yu, Polyhedral-aupd nanoparticles-based dual-mode cytosensor with turn on enable signal for highly sensitive cell evaluation on lab-on-paper device. *Biosens. Bioelectron.* **117**, 651–658 (2018)
100. M. Moazeni, F. Karimzadeh, A. Kermanpur, Peptide modified paper based impedimetric immunoassay with nanocomposite electrodes as a point-of-care testing of alpha-fetoprotein in human serum. *Biosens. Bioelectron.* **117**, 748–757 (2018)
101. J. Qi, B. Li, N. Zhou, X. Wang, D. Deng, L. Luo, L. Chen, The strategy of antibody-free biomarker analysis by in-situ synthesized molecularly imprinted polymers on movable valve paper-based device. *Biosensors and Bioelectronics* **142**, 111,533 (2019)
102. T. He, J. Li, L. Liu, S. Ge, M. Yan, H. Liu, J. Yu, Origami-based “book” shaped three-dimensional electrochemical paper microdevice for sample-to-answer

- detection of pathogens. *RSC Adv.* **10**(43), 25808–25816 (2020)
103. M. Santhiago, C.S. Henry, L.T. Kubota, Low cost, simple three dimensional electrochemical paper-based analytical device for determination of p-nitrophenol. *Electrochim. Acta* **130**, 771–777 (2014)
 104. S. Boonkaew, I. Jang, E. Noviana, W. Siangproh, O. Chailapakul, C.S. Henry, Electrochemical paper-based analytical device for multiplexed, point-of-care detection of cardiovascular disease biomarkers. *Sensors and Actuators B: Chemical* **330**, 129,336 (2021)
 105. A. Yakoh, S. Chaiyo, W. Siangproh, O. Chailapakul, 3d capillary-driven paper-based sequential microfluidic device for electrochemical sensing applications. *ACS sensors* **4**(5), 1211–1221 (2019)
 106. L. Wang, B. Li, J. Wang, J. Qi, J. Li, J. Ma, L. Chen, A rotary multi-positioned cloth/paper hybrid microfluidic device for simultaneous fluorescence sensing of mercury and lead ions by using ion imprinted technologies. *Journal of Hazardous Materials* **428**, 128,165 (2022)
 107. Y. Zhu, X. Tong, Q. Wei, G. Cai, Y. Cao, C. Tong, S. Shi, F. Wang, 3d origami paper-based ratiometric fluorescent microfluidic device for visual point-of-care detection of alkaline phosphatase and butyrylcholinesterase. *Biosensors and Bioelectronics* **196**, 113,691 (2022)
 108. L. Shi, L. Li, X. Li, G. Zhang, Y. Zhang, C. Dong, S. Shuang, Excitation-independent yellow-fluorescent nitrogen-doped carbon nanodots for biological imaging and paper-based sensing. *Sens. Actuators, B Chem.* **251**, 234–241 (2017)
 109. L. Zong, Y. Xie, Q. Li, Z. Li, A new red fluorescent probe for hg²⁺ based on naphthalene diimide and its application in living cells, reversibility on strip papers. *Sens. Actuators, B Chem.* **238**, 735–743 (2017)
 110. C. Liu, D. Ning, C. Zhang, Z. Liu, R. Zhang, J. Zhao, T. Zhao, B. Liu, Z. Zhang, Dual-colored carbon dot ratiometric fluorescent test paper based on a specific spectral energy transfer for semiquantitative assay of copper ions. *ACS Applied Materials & Interfaces* **9**(22), 18897–18903 (2017)
 111. N. Nuchtavorn, M. Macka, A novel highly flexible, simple, rapid and low-cost fabrication tool for paper-based microfluidic devices (μ pads) using technical drawing pens and in-house formulated aqueous inks. *Anal. Chim. Acta* **919**, 70–77 (2016)
 112. J. Yu, L. Ge, J. Huang, S. Wang, S. Ge, Microfluidic paper-based chemiluminescence biosensor for simultaneous determination of glucose and uric acid. *Lab Chip* **11**(7), 1286–1291 (2011)
 113. J. Yu, S. Wang, L. Ge, S. Ge, A novel chemiluminescence paper microfluidic biosensor based on enzymatic reaction for uric acid determination. *Biosens. Bioelectron.* **26**(7), 3284–3289 (2011)
 114. I. Al Yahyai, H.A. Al-Lawati, J. Hassanzadeh, Carbon dots-modified paper-based chemiluminescence device for rapid determination of mercury (ii) in cosmetics. *Luminescence* (2022)
 115. M. Zangheri, L. Cevenini, L. Anfossi, C. Baggiani, P. Simoni, F. Di Nardo, A. Roda, A simple and compact smartphone accessory for quantitative chemiluminescence-based lateral flow immunoassay for salivary cortisol detection. *Biosens. Bioelectron.* **64**, 63–68 (2015)
 116. A.K. Yetisen, M.S. Akram, C.R. Lowe, based microfluidic point-of-care diagnostic devices. *Lab Chip* **13**(12), 2210–2251 (2013)
 117. J.L. Delaney, C.F. Hogan, J. Tian, W. Shen, Electrogenerated chemiluminescence detection in paper-based microfluidic sensors. *Anal. Chem.* **83**(4), 1300–1306 (2011)
 118. L. Wu, C. Ma, X. Zheng, H. Liu, J. Yu, based electrochemiluminescence origami device for protein detection using assembled cascade dna-carbon dots nanotags based on rolling circle amplification. *Biosens. Bioelectron.* **68**, 413–420 (2015)
 119. L. Ge, J. Yan, X. Song, M. Yan, S. Ge, J. Yu, Three-dimensional paper-based electrochemiluminescence immunodevice for multiplexed measurement of biomarkers and point-of-care testing. *Biomaterials* **33**(4), 1024–1031 (2012)
 120. J. Yan, L. Ge, X. Song, M. Yan, S. Ge, J. Yu, Paper-based electrochemiluminescent 3d immunodevice for lab-on-paper, specific, and sensitive point-of-care testing. *Chemistry-A European Journal* **18**(16), 4938–4945 (2012)
 121. J. Cai, T. Jin, J. Kou, S. Zou, J. Xiao, Q. Meng, Lucas-washburn equation-based modeling of capillary-driven flow in porous systems. *Langmuir* **37**(5), 1623–1636 (2021)
 122. A. Ponomarenko, D. Quéré, C. Clanet, A universal law for capillary rise in corners. *J. Fluid Mech.* **666**, 146–154 (2011)
 123. N. Fries, M. Dreyer, An analytic solution of capillary rise restrained by gravity. *J. Colloid Interface Sci.* **320**(1), 259–263 (2008)
 124. S. Patari, P.S. Mahapatra, Liquid wicking in a paper strip: An experimental and numerical study. *ACS Omega* **5**(36), 22931–22939 (2020)
 125. S. Bhattacharya, S. Kumar, A.K. Agarwal, *Paper microfluidics* (Springer, 2019)
 126. Y. Wang, D. Ye, X. Zhu, Y. Yang, C. Qin, R. Chen, Q. Liao, Spontaneous imbibition in paper-based microfluidic devices: Experiments and numerical simulations. *Langmuir* **38**(8), 2677–2685 (2022)
 127. R. Masoodi, H. Tan, K.M. Pillai, Darcy’s law-based numerical simulation for modeling 3d liquid absorption into porous wicks. *AIChE J.* **57**(5), 1132–1143 (2011)
 128. Z. Liu, J. Hu, Y. Zhao, Z. Qu, F. Xu, Experimental and numerical studies on liquid wicking into filter papers for paper-based diagnostics. *Appl. Therm. Eng.* **88**, 280–287 (2015)
 129. T. Ouyang, J. Lu, P. Xu, X. Hu, J. Chen, Mechanism study and evaluation of high efficiency paper-based microfluidic fuel cell coupled with capillary force. *Journal of Power Sources* **520**, 230,807 (2022)
 130. S. Modha, Control and modeling of imbibition in paper-based microfluidic devices. Ph.D. thesis, University of California, Riverside (2022)
 131. E. Elizalde, R. Urteaga, C.L. Berli, Rational design of capillary-driven flows for paper-based microfluidics. *Lab Chip* **15**(10), 2173–2180 (2015)

132. J. Songok, M. Toivakka, Modelling of capillary-driven flow for closed paper-based microfluidic channels. *Journal of Micromechanics and Microengineering* **27**(6), 065,001 (2017)
133. T. Rosenfeld, M. Bercovici, 1000-fold sample focusing on paper-based microfluidic devices. *Lab Chip* **14**(23), 4465–4474 (2014)
134. V. Dushin, N. Smirnov, V. Nikitin, E. Skryleva, Y.G. Weisman, Multiple capillary-driven imbibition of a porous medium under microgravity conditions: Experimental investigation and mathematical modeling. *Acta Astronaut.* **193**, 572–578 (2022)
135. P.A. More, P.V. Tandel, Study of parametric effect on saturation rate in imbibition phenomenon for various porous materials. *Journal of Ocean Engineering and Science* (2022)
136. Q. Meng, L. Zhao, P. Li, F. Yang, J. Cai, Experiments and phase-field simulation of counter-current imbibition in porous media with different pore structure. *Journal of Hydrology* **608**, 127,670 (2022)
137. W. Wang, L.L. Shen, H. Yu, W. Xu, J. Wang, C. Yong, G.R. Zhang, D. Mei, Solar-boosted paper-based microfluidic fuel cells for miniaturized power sources. *Advanced Materials Technologies* p. 2200154 (2022)
138. T. Songjaroen, W. Dungchai, O. Chailapakul, C.S. Henry, W. Laiwattanapaisal, Blood separation on microfluidic paper-based analytical devices. *Lab Chip* **12**(18), 3392–3398 (2012)
139. J. Noiphung, T. Songjaroen, W. Dungchai, C.S. Henry, O. Chailapakul, W. Laiwattanapaisal, Electrochemical detection of glucose from whole blood using paper-based microfluidic devices. *Anal. Chim. Acta* **788**, 39–45 (2013)
140. X. Yang, O. Forouzan, T.P. Brown, S.S. Shevkopyas, Integrated separation of blood plasma from whole blood for microfluidic paper-based analytical devices. *Lab Chip* **12**(2), 274–280 (2012)
141. S. Kar, T.K. Maiti, S. Chakraborty, Capillarity-driven blood plasma separation on paper-based devices. *Analyst* **140**(19), 6473–6476 (2015)
142. D. Kim, S. Kim, S. Kim, An innovative blood plasma separation method for a paper-based analytical device using chitosan functionalization. *Analyst* **145**(16), 5491–5499 (2020)
143. F. Burgos-Flórez, A. Rodríguez, E. Cervera, M. De Ávila, M. Sanjuán, P.J. Villalba, Microfluidic paper-based blood plasma separation device as a potential tool for timely detection of protein biomarkers. *Micromachines* **13**(5), 706 (2022)
144. G. Daniels, I. Bromilow, *Essential guide to blood groups* (John Wiley & Sons, 2011)
145. D. Proverbio, E. Spada, L. Baggiani, R. Perego, Assessment of a gel column technique for feline blood typing. *Vet. Res. Commun.* **33**(1), 201–203 (2009)
146. M. Ota, H. Fukushima, I. Yonemura, H. Hasekura, Detection of ab0 blood group-active glycolipids extracted from red cell membrane and heat hematoma using tlc-immunostaining. *Z. Rechtsmed.* **100**(2), 215–221 (1988)
147. M.S. Khan, G. Thouas, W. Shen, G. Whyte, G. Garnier, Paper diagnostic for instantaneous blood typing. *Anal. Chem.* **82**(10), 4158–4164 (2010)
148. P. Jarujamrus, J. Tian, X. Li, A. Siripinyanond, J. Shiowatana, W. Shen, Mechanisms of red blood cells agglutination in antibody-treated paper. *Analyst* **137**(9), 2205–2210 (2012)
149. N. Larpant, W. Niamsi, J. Noiphung, W. Chanakiat, T. Sakuldamrongpanich, V. Kittichai, T. Tongloy, S. Chuwongin, S. Boonsang, W. Laiwattanapaisal, Simultaneous phenotyping of five rh red blood cell antigens on a paper-based analytical device combined with deep learning for rapid and accurate interpretation. *Analytica Chimica Acta* **1207**, 339,807 (2022)
150. T. Pasinszki, M. Krebsz, Biosensors for non-invasive detection of celiac disease biomarkers in body fluids. *Biosensors* **8**(2), 55 (2018)
151. P.M. Kouw, P.M. de Vries, A.J. Donker, Non-invasive measurement of body fluid dynamics. *Int. Yearb. Nephrol.* **1993**, 333–351 (1992)
152. C. Olthof, P. De Vries, P. Kouw, P. Oe, H. Schneider, J. De Lange, A. Donker, Non-invasive conductivity method for detection of dynamic body fluid changes: in vitro and in vivo validation. *Nephrol. Dial. Transplant.* **8**(1), 41–46 (1993)
153. S. Dalirirad, A.J. Steckl, Lateral flow assay using aptamer-based sensing for on-site detection of dopamine in urine. *Analytical biochemistry* **596**, 113,637 (2020)
154. J.E. Schonhorn, S.C. Fernandes, A. Rajaratnam, R.N. Deraney, J.P. Rolland, C.R. Mace, A device architecture for three-dimensional, patterned paper immunoassays. *Lab Chip* **14**(24), 4653–4658 (2014)
155. L. Xiao, Z. Zhang, C. Wu, L. Han, H. Zhang, Molecularly imprinted polymer grafted paper-based method for the detection of 17 β -estradiol. *Food Chem.* **221**, 82–86 (2017)
156. J.M. Bauça, E. Martínez-Morillo, E.P. Diamandis, Peptidomics of urine and other biofluids for cancer diagnostics. *Clin. Chem.* **60**(8), 1052–1061 (2014)
157. A. Beaucamp, M. Culebras, M.N. Collins, Sustainable mesoporous carbon nanostructures derived from lignin for early detection of glucose. *Green Chem.* **23**(15), 5696–5705 (2021)
158. S. Hu, J.A. Loo, D.T. Wong, Human body fluid proteome analysis. *Proteomics* **6**(23), 6326–6353 (2006)
159. D. Pérez, J. Orozco, Wearable electrochemical biosensors to measure biomarkers with complex blood-to-sweat partition such as proteins and hormones. *Microchim. Acta* **189**(3), 1–28 (2022)
160. J.M. Bhagu, Probing the in-situ conformation of monoclonal antibodies at hydrophobic interfaces using nmr spectroscopy. Ph.D. thesis, Florida Agricultural and Mechanical University (2021)
161. B. Veerabhadrapa, C. Delaby, C. Hirtz, J. Vialaret, D. Alcolea, A. Lleó, J. Fortea, M.S. Santosh, S. Choubey, S. Lehmann, Detection of amyloid beta peptides in body fluids for the diagnosis of alzheimer's disease: Where do we stand? *Crit. Rev. Clin. Lab. Sci.* **57**(2), 99–113 (2020)
162. P. Rattanarat, W. Dungchai, W. Siangproh, O. Chailapakul, C.S. Henry, Sodium dodecyl sulfate-modified electrochemical paper-based analytical device for determination of dopamine levels in biological samples. *Anal. Chim. Acta* **744**, 1–7 (2012)

163. X.Y. Shao, C.R. Wang, C.M. Xie, X.G. Wang, R.L. Liang, W.W. Xu, Rapid and sensitive lateral flow immunoassay method for procalcitonin (pct) based on time-resolved immunochromatography. *Sensors* **17**(3), 480 (2017)
164. S. Kasetsirikul, M. Umer, N. Soda, K.R. Sreejith, M.J. Shiddiky, N.T. Nguyen, Detection of the sars-cov-2 humanized antibody with paper-based elisa. *Analyst* **145**(23), 7680–7686 (2020)
165. T. Yang, Y.C. Wang, C.F. Shen, C.M. Cheng. Point-of-care rna-based diagnostic device for covid-19 (2020)
166. M. Kumar, S. Gulati, A.H. Ansari, R. Phutela, S. Acharya, M. Azhar, J. Murthy, P. Kathpalia, A. Kanakan, R. Maurya, et al., Fncas9-based crispr diagnostic for rapid and accurate detection of major sars-cov-2 variants on a paper strip. *Elife* **10**, e67,130 (2021)
167. F. Gong, H.x. Wei, J. Qi, H. Ma, L. Liu, J. Weng, X. Zheng, Q. Li, D. Zhao, H. Fang, et al., Pulling-force spinning top for serum separation combined with paper-based microfluidic devices in covid-19 elisa diagnosis. *ACS sensors* **6**(7), 2709–2719 (2021)
168. Y. Ming, S. Hao, F. Wang, Y.R. Lewis-Israeli, B.D. Volmert, Z. Xu, A. Goestenkers, A. Aguirre, C. Zhou, Longitudinal morphological and functional characterization of human heart organoids using optical coherence tomography. *Biosensors and Bioelectronics* **207**, 114,136 (2022)
169. D. Liu, C. Ju, C. Han, R. Shi, X. Chen, D. Duan, J. Yan, X. Yan, Nanozyme chemiluminescence paper test for rapid and sensitive detection of sars-cov-2 antigen. *Biosensors and Bioelectronics* **173**, 112,817 (2021)
170. A.A. Weaver, H. Reiser, T. Barstis, M. Benvenuti, D. Ghosh, M. Hunckler, B. Joy, L. Koenig, K. Raddell, M. Lieberman, Paper analytical devices for fast field screening of beta lactam antibiotics and antituberculosis pharmaceuticals. *Anal. Chem.* **85**(13), 6453–6460 (2013)
171. M.T. Koesdjojo, Y. Wu, A. Boonloed, E.M. Dunfield, V.T. Remcho, Low-cost, high-speed identification of counterfeit antimalarial drugs on paper. *Talanta* **130**, 122–127 (2014)
172. K. Kaarj, P. Akarapipad, J.Y. Yoon, Simpler, faster, and sensitive zika virus assay using smartphone detection of loop-mediated isothermal amplification on paper microfluidic chips. *Sci. Rep.* **8**(1), 1–11 (2018)
173. X. Ye, J. Xu, L. Lu, X. Li, X. Fang, J. Kong, Equipment-free nucleic acid extraction and amplification on a simple paper disc for point-of-care diagnosis of rotavirus a. *Anal. Chim. Acta* **1018**, 78–85 (2018)
174. S.T. Mensah, Y. Gonzalez, P. Calvo-Marzal, K.Y. Chumbimuni-Torres, Nanomolar detection limits of cd2+, ag+, and k+ using paper-strip ion-selective electrodes. *Anal. Chem.* **86**(15), 7269–7273 (2014)
175. P. Yu, C.A. Heist, V.T. Remcho, A novel laminated polycaprolactone/paper/silver electrode for lead (ii) detection. *Anal. Methods* **9**(11), 1702–1706 (2017)
176. X. Wang, J. Sun, J. Tong, X. Guan, C. Bian, S. Xia, based sensor chip for heavy metal ion detection by swsv. *Micromachines* **9**(4), 150 (2018)
177. F.M. Shimizu, A.M. Pasqualetti, C.Y. Nicoliche, A.L. Gobbi, M. Santhiago, R.S. Lima, Alcohol-triggered capillarity through porous pyrolyzed paper-based electrodes enables ultrasensitive electrochemical detection of phosphate. *ACS sensors* **6**(8), 3125–3132 (2021)
178. A. Cioffi, M. Mancini, V. Gioia, S. Cinti, Office paper-based electrochemical strips for organophosphorus pesticide monitoring in agricultural soil. *Environmental Science & Technology* **55**(13), 8859–8865 (2021)
179. M.L. Scala-Benuzzi, J. Raba, G.J. Soler-Illia, R.J. Schneider, G.A. Messina, Novel electrochemical paper-based immunocapture assay for the quantitative determination of ethinylestradiol in water samples. *Anal. Chem.* **90**(6), 4104–4111 (2018)
180. E. Costa-Rama, H. Nouws, C. Delerue-Matos, M.d.C. Blanco-López, M.T. Fernández-Abedul, Preconcentration and sensitive determination of the anti-inflammatory drug diclofenac on a paper-based electroanalytical platform. *Analytica Chimica Acta* **1074**, 89–97 (2019)
181. H. Guo, M.H. Yeh, Y. Zi, Z. Wen, J. Chen, G. Liu, C. Hu, Z.L. Wang, Ultralight cut-paper-based self-charging power unit for self-powered portable electronic and medical systems. *ACS Nano* **11**(5), 4475–4482 (2017)
182. Y. Liu, K. Cui, Q. Kong, L. Zhang, S. Ge, J. Yu, A self-powered origami paper analytical device with a pop-up structure for dual-mode electrochemical sensing of atp assisted by glucose oxidase-triggered reaction. *Biosensors and Bioelectronics* **148**, 111,839 (2020)
183. H. Lee, S. Choi, An origami paper-based bacteria-powered battery. *Nano Energy* **15**, 549–557 (2015)
184. L.L. Shen, G.R. Zhang, M. Biesalski, B.J. Etzold, based microfluidic aluminum-air batteries: toward next-generation miniaturized power supply. *Lab Chip* **19**(20), 3438–3447 (2019)
185. Y. Wang, H.Y. Kwok, W. Pan, H. Zhang, X. Lu, D.Y. Leung, Parametric study and optimization of a low-cost paper-based al-air battery with corrosion inhibition ability. *Applied Energy* **251**, 113,342 (2019)
186. Y. Yang, H. Zhang, X. Zhu, D. Ye, R. Chen, Q. Liao, A hollow structure for flow and bendable paper-based zinc-air battery. *International Journal of Energy Research* (2022)
187. A. Zebda, L. Renaud, M. Cretin, F. Pichot, C. Innocent, R. Ferrigno, S. Tingry, A microfluidic glucose biofuel cell to generate micropower from enzymes at ambient temperature. *Electrochem. Commun.* **11**(3), 592–595 (2009)
188. H.B. Noh, Y.B. Shim, Catalytic activity of polymerized self-assembled artificial enzyme nanoparticles: applications to microfluidic channel-glucose biofuel cells and sensors. *Journal of Materials Chemistry A* **4**(7), 2720–2728 (2016)
189. R.K. Arun, S. Halder, N. Chanda, S. Chakraborty, A paper based self-pumping and self-breathing fuel cell using pencil stroked graphite electrodes. *Lab Chip* **14**(10), 1661–1664 (2014)
190. T.M. Cardoso, P.T. Garcia, W.K. Coltro, Colorimetric determination of nitrite in clinical, food and environmental samples using microfluidic devices stamped in paper platforms. *Anal. Methods* **7**(17), 7311–7317 (2015)
191. E. Trofimchuk, Y. Hu, A. Nilghaz, M.Z. Hua, S. Sun, X. Lu, Development of paper-based microfluidic device

- for the determination of nitrite in meat. *Food chemistry* **316**, 126,396 (2020)
192. X. Hu, L. Lu, C. Fang, B. Duan, Z. Zhu, Determination of apparent amylose content in rice by using paper-based microfluidic chips. *J. Agric. Food Chem.* **63**(44), 9863–9868 (2015)
 193. S.A. Nogueira, A.D. Lemes, A.C. Chagas, M.L. Vieira, M. Talhavini, P.A. Morais, W.K. Coltro, Redox titration on foldable paper-based analytical devices for the visual determination of alcohol content in whiskey samples. *Talanta* **194**, 363–369 (2019)
 194. S. Patari, P.S. Mahapatra, in *2021 IEEE Sensors (IEEE, 2021)*, pp. 1–4
 195. B.G. Guinati, L.R. Sousa, K.A. Oliveira, W.K. Coltro, Simultaneous analysis of multiple adulterants in milk using microfluidic paper-based analytical devices. *Anal. Methods* **13**(44), 5383–5390 (2021)
 196. M. Dong, J. Wu, Z. Ma, H. Peretz-Soroka, M. Zhang, P. Komenda, N. Tangri, Y. Liu, C. Rigatto, F. Lin, Rapid and low-cost crp measurement by integrating a paper-based microfluidic immunoassay with smartphone (crp-chip). *Sensors* **17**(4), 684 (2017)
 197. S.A. Bhakta, R. Borba, M. Taba Jr., C.D. Garcia, E. Carrillo, Determination of nitrite in saliva using microfluidic paper-based analytical devices. *Anal. Chim. Acta* **809**, 117–122 (2014)
 198. R. Menger, M. Bontha, J. Beveridge, T. Borch, C. Henry, Fluorescent dye paper-based method for assessment of pesticide coverage on leaves and trees: a citrus grove case study. *J. Agric. Food Chem.* **68**(47), 14009–14014 (2020)
 199. D. Jiang, P. Ge, L. Wang, H. Jiang, M. Yang, L. Yuan, Q. Ge, W. Fang, X. Ju, A novel electrochemical mast cell-based paper biosensor for the rapid detection of milk allergen casein. *Biosens. Bioelectron.* **130**, 299–306 (2019)
 200. M. Srisa-Art, K.E. Boehle, B.J. Geiss, C.S. Henry, Highly sensitive detection of salmonella typhimurium using a colorimetric paper-based analytical device coupled with immunomagnetic separation. *Anal. Chem.* **90**(1), 1035–1043 (2018)
 201. C. Srisomwat, P. Teengam, N. Chuaypen, P. Tangkijvanich, T. Vilaivan, O. Chailapakul, Pop-up paper electrochemical device for label-free hepatitis b virus dna detection. *Sensors and Actuators B: Chemical* **316**, 128,077 (2020)
 202. T.N. Jilani, R.T. Jamil, A.H. Siddiqui, *H1n1 influenza (swine flu)* (StatPearls, Treasure Island (FL), 2020)
 203. M.P. Nguyen, S.P. Kelly, J.B. Wydallis, C.S. Henry, Read-by-eye quantification of aluminum (iii) in distance-based microfluidic paper-based analytical devices. *Anal. Chim. Acta* **1100**, 156–162 (2020)
 204. J. Reboud, G. Xu, A. Garrett, M. Adriko, Z. Yang, E.M. Tukahebwa, C. Rowell, J.M. Cooper, based microfluidics for dna diagnostics of malaria in low resource underserved rural communities. *Proc. Natl. Acad. Sci.* **116**(11), 4834–4842 (2019)
 205. S. Ardalan, M. Hosseinifard, M. Vosough, H. Golmohammadi, Towards smart personalized perspiration analysis: An iot-integrated cellulose-based microfluidic wearable patch for smartphone fluorimetric multi-sensing of sweat biomarkers. *Biosensors and Bioelectronics* **168**, 112,450 (2020)
 206. A. Kaushik, S. Tiwari, R.D. Jayant, A. Marty, M. Nair, Towards detection and diagnosis of ebola virus disease at point-of-care. *Biosens. Bioelectron.* **75**, 254–272 (2016)
 207. L. Cao, C. Fang, R. Zeng, X. Zhao, Y. Jiang, Z. Chen, based microfluidic devices for electrochemical immunofiltration analysis of human chorionic gonadotropin. *Biosens. Bioelectron.* **92**, 87–94 (2017)
 208. M.M. Honikel, C.E. Lin, B.A. Cardinell, J.T. LaBelle, A.D. Penman, Direct measurement of a biomarker's native optimal frequency with physical adsorption based immobilization. *ACS sensors* **3**(4), 823–831 (2018)
 209. D. Thompson, Y. Lei, Mini review: Recent progress in rt-lamp enabled covid-19 detection. *Sensors and Actuators Reports* **2**(1), 100,017 (2020)
 210. J.P. Broughton, X. Deng, G. Yu, C.L. Fasching, J. Singh, J. Streithorst, A. Granados, A. Sotomayor-Gonzalez, K. Zorn, A. Gopez, et al., Rapid detection of 2019 novel coronavirus sars-cov-2 using a crispr-based detectr lateral flow assay. *MedRxiv* (2020)
 211. Q. Hui, Y. Pan, Z. Yang, based devices for rapid diagnostics and testing sewage for early warning of covid-19 outbreak. *Case Studies in Chemical and Environmental Engineering* **2**, 100,064 (2020)
 212. R. Suvanasuthi, S. Chinnaronk, C. Promptmas, 3d printed hydrophobic barriers in a paper-based biosensor for point-of-care detection of dengue virus serotypes. *Talanta* **237**, 122,962 (2022)
 213. P. Mufidah Sari, A. Daud, H. Sulistyarti, A. Sabarudin, D. Nacapricha, An application study of membraneless-gas separation microfluidic paper-based analytical device for monitoring total ammonia in fish pond water using natural reagent. *Analytical Sciences* **38**(5), 759–767 (2022)
 214. O. Amor-Gutiérrez, E. Costa-Rama, M.T. Fernández-Abedul, Fully integrated sampler and dilutor in an electrochemical paper-based device for glucose sensing. *Microchim. Acta* **188**(9), 1–8 (2021)
 215. A. Pal, H.E. Cuellar, R. Kuang, H.F. Caurin, D. Goswami, R.V. Martinez, Self-powered, paper-based electrochemical devices for sensitive point-of-care testing. *Advanced materials technologies* **2**(10), 1700,130 (2017)
 216. T. Komatsu, R.R. Gabatino, H. Hofleña, M. Maeki, A. Ishida, H. Tani, M. Tokeshi, Using a paper-based analytical device designed for remote learning environments to achieve simple quantitative colorimetry without micropipettes. *J. Chem. Educ.* **98**(9), 3050–3054 (2021)
 217. P. Yomthiangthae, O. Chailapakul, W. Siangproh, Rapid urinary albumin detection using a simple redox cycling process coupled with a paper-based device. *Journal of Electroanalytical Chemistry* **911**, 116,230 (2022)
 218. S. Patari, P. Datta, P.S. Mahapatra, 3d paper-based milk adulteration detection device. *Sci. Rep.* **12**(1), 1–14 (2022)
 219. J. Zhao, Y. Zhang, F. Liu, M. Yan, X. Wang, W. Wang, Sunlight-responsive titania-hydrated tungsten oxide heteronanoparticles/paper-based color-switching film for solar ultraviolet radiation monitors. *ACS Applied Nano Materials* **5**(3), 4009–4017 (2022)

220. E. Ghohestani, J. Tashkhourian, B. Hemmateenejad, Colorimetric determination of peroxide value in vegetable oils using a paper based analytical device. *Food Chemistry* p. 134345 (2022)
221. D. Maier, E. Laubender, A. Basavanna, S. Schumann, F. Guder, G.A. Urban, C. Dincer, Toward continuous monitoring of breath biochemistry: a paper-based wearable sensor for real-time hydrogen peroxide measurement in simulated breath. *ACS sensors* **4**(11), 2945–2951 (2019)
222. M. Asif, F.R. Awan, Q.M. Khan, B. Ngamsom, N. Pamme, based analytical devices for colorimetric detection of *s. aureus* and *e. coli* and their antibiotic resistant strains in milk. *Analyst* **145**(22), 7320–7329 (2020)
223. B. O’Farrell, in *Lateral flow immunoassay* (Springer, 2009), pp. 1–33

Springer Nature or its licensor (e.g. a society or other partner) holds exclusive rights to this article under a publishing agreement with the author(s) or other rightsholder(s); author self-archiving of the accepted manuscript version of this article is solely governed by the terms of such publishing agreement and applicable law.